Title

Human Epitopes Identified from Herpes Simplex Virus Tegument Protein VP11/12 (UL46) Recall Multifunctional Effector Memory CD4+ TEM Cells in Asymptomatic Individuals and Protect from Ocular Herpes Infection and Disease in "Humanized" HLA-DR Transgeni...

Journal

Journal of Virology, 94(7)

ISSN

0022-538X

Authors

Srivastava, Ruchi
Coulon, Pierre-Gregoire A
Prakash, Swayam
et al.

Publication Date

2020-03-17

DOI

10.1128/jvi.01991-19

Peer reviewed

AMERICAN SOCIETY FOR MICROBIOLOGY | Journal of Virology®

CELLULAR RESPONSE TO INFECTION

Human Epitopes Identified from Herpes Simplex Virus Tegument Protein VP11/12 (UL46) Recall Multifunctional Effector Memory CD4$^+$ T_{EM} Cells in Asymptomatic Individuals and Protect from Ocular Herpes Infection and Disease in "Humanized" HLA-DR Transgenic Mice

Ruchi Srivastava,[a] Pierre-Gregoire A. Coulon,[a] Swayam Prakash,[a] Nisha R. Dhanushkodi,[a] Soumyabrata Roy,[a] Angela M. Nguyen,[a] Nuha I. Alomari,[a] Uyen T. Mai,[a] Cassendra Amezquita,[a] Caitlin Ye,[a] Bernard Maillère,[b] Lbachir BenMohamed[a,c,d]

[a]Laboratory of Cellular and Molecular Immunology, Gavin Herbert Eye Institute, University of California Irvine, School of Medicine, Irvine, California, USA
[b]Commissariat à l'Energie Atomique et aux Energies Alternatives-Saclay, Université Paris-Saclay, Service d'Ingénierie Moléculaire des Protéines, Gif-sur-Yvette, France
[c]Department of Molecular Biology and Biochemistry, University of California Irvine, School of Medicine, Irvine, California, USA
[d]Institute for Immunology, University of California Irvine, School of Medicine, Irvine, California, USA

ABSTRACT While the role of CD8$^+$ T cells in the control of herpes simplex virus 1 (HSV-1) infection and disease is gaining wider acceptance, a direct involvement of effector CD4$^+$ T cells in this protection and the phenotype and function of HSV-specific human CD4$^+$ T cell epitopes remain to be fully elucidated. In the present study, we report that several epitopes from the HSV-1 virion tegument protein (VP11/12) encoded by UL46 are targeted by CD4$^+$ T cells from HSV-seropositive asymptomatic individuals (who, despite being infected, never develop any recurrent herpetic disease). Among these, we identified two immunodominant effector memory CD4$^+$ T_{EM} cell epitopes, amino acids (aa) 129 to 143 of VP11/12 (VP11/12$_{129-143}$) and VP11/12$_{483-497}$, using *in silico*, *in vitro*, and *in vivo* approaches based on the following: (i) a combination of the TEPITOPE algorithm and PepScan library scanning of the entire 718 aa of HSV-1 VP11/12 sequence; (ii) an *in silico* peptide-protein docking analysis and *in vitro* binding assay that identify epitopes with high affinity to soluble HLA-DRB1 molecules; and (iii) an ELISpot assay and intracellular detection of gamma interferon (IFN-γ), CD107$^{a/b}$ degranulation, and CD4$^+$ T cell carboxyfluorescein succinimidyl ester (CFSE) proliferation assays. We demonstrated that native VP11/12$_{129-143}$ and VP11/12$_{483-497}$ epitopes presented by HSV-1-infected HLA-DR-positive target cells were recognized mainly by effector memory CD4$^+$ T_{EM} cells while being less targeted by FOXP3$^+$ CD4$^+$ CD25$^+$ regulatory T cells. Furthermore, immunization of HLA-DR transgenic mice with a mixture of the two immunodominant human VP11/12 CD4$^+$ T_{EM} cell epitopes, but not with cryptic epitopes, induced HSV-specific polyfunctional IFN-γ-producing CD107^{ab+} CD4$^+$ T cells associated with protective immunity against ocular herpes infection and disease.

IMPORTANCE We report that naturally protected HSV-1-seropositive asymptomatic individuals develop a higher frequency of antiviral effector memory CD4$^+$ T_{EM} cells specific to two immunodominant epitopes derived from the HSV-1 tegument protein VP11/12. Immunization of HLA-DR transgenic mice with a mixture of these two immunodominant CD4$^+$ T cell epitopes induced a robust antiviral CD4$^+$ T cell response in the cornea that was associated with protective immunity against ocular herpes. The emerging concept of developing an asymptomatic herpes vaccine that would boost effector memory CD4$^+$ and CD8$^+$ T_{EM} cell responses is discussed.

Citation Srivastava R, Coulon P-GA, Prakash S, Dhanushkodi NR, Roy S, Nguyen AM, Alomari NI, Mai UT, Amezquita C, Ye C, Maillère B, BenMohamed L. 2020. Human epitopes identified from herpes simplex virus tegument protein VP11/12 (UL46) recall multifunctional effector memory CD4$^+$ T_{EM} cells in asymptomatic individuals and protect from ocular herpes infection and disease in "humanized" HLA-DR transgenic mice. J Virol 94:e01991-19. https://doi.org/10.1128/JVI.01991-19.

Editor Jae U. Jung, University of Southern California

Address correspondence to Lbachir BenMohamed, Lbenmoha@uci.edu.

Received 25 November 2019
Accepted 2 January 2020
Accepted manuscript posted online 8 January 2020
Published 17 March 2020

KEYWORDS CD4$^+$ T cells, HLA transgenic mice, HSV-1, UL46, VP11/12, epitope, human, mapping, tegument protein

A staggering 3.72 billion individuals worldwide currently carry herpes simplex virus 1 (HSV-1), which causes a wide range of diseases throughout their lives (1). Ocular herpes, caused by HSV-1, is a potentially blinding disease impacting over 450,000 individuals in the United States (2–5). Current antiviral drug therapies (e.g., acyclovir and derivatives) reduce recurrent herpetic disease by ~45% but does not eliminate the virus (6, 7). One such powerful and cost-effective strategy would be an effective vaccine able to eliminate the virus and the root of the disease as a means to prevent corneal herpetic disease and blindness (7–9).

There is substantial literature currently on the role of CD8$^+$ T cells in the protection against herpes, whereas the role of CD4$^+$ T cells in such protection is relatively less known (10–14). Activated CD4$^+$ T cells are retained in latently infected trigeminal ganglia (TG) of mice and humans. In addition to their direct effect on virus replication, the CD4$^+$ T helper cells are a source of large amounts of cytokines that promote the generation of primary and memory CD8$^+$ T cell responses, thus indirectly contributing to protection (15, 16). Given the significant role of CD4$^+$ T cells in herpes virus immunity, the identification and characterization of CD4$^+$ T cell epitopes are crucial steps toward the design of an epitope-based herpes vaccine.

Several unsuccessful attempts to develop a herpes vaccine have concentrated around HSV glycoproteins (17–20). The HSV-1 and HSV-2 experimental vaccines designed to date were either purified virion products derived from infected cells (subunit vaccines), purified recombinant immunogenic HSV-coded proteins, focused mainly on the glycoprotein gD or attenuated live viruses lacking some of the virulence features, such as gH and gE (17, 21). The most prevalent CD4$^+$ T cell responses in HSV-seropositive humans were detected against tegument proteins (22), suggesting their importance in preventing the infection. Tegument proteins are functional molecules located between the viral capsid enveloping the genome and the outer membrane (22–25). Previous reports have indicated that the genes encoding the tegument proteins are conserved between HSV-1 and HSV-2 and possess a high degree of similarity in viruses in the alpha subfamily. The tegument virion protein 11/12 (VP11/12) is encoded by the HSV open reading frame (ORF) *UL46*. Notably, CD4$^+$ T cells from infected humans recognize a couple of epitopes in HSV-2 VP11/12 (26–28). However, the complete repertoire of HSV-1 VP11/12 CD4$^+$ T cell epitopes remains to be fully elucidated.

In this study, we followed several *in silico*, *in vitro*, and *in vivo* epitope mapping approaches to identify the CD4$^+$ T cell epitopes from the HSV-1 VP11/12. We discovered frequent, robust, and polyfunctional effector memory CD4$^+$ T_{EM} cell responses directed predominantly against two human epitopes, residues 129 to 143 of VP11/12 (VP11/12$_{129-143}$) and VP11/12$_{483-497}$, among HSV-seropositive healthy asymptomatic individuals. We further validated this finding in a "humanized" transgenic HLA-DR mouse model of ocular herpes by observing strong protective immunity associated with robust and polyfunctional VP11/12 epitope-specific CD4$^+$ T cell responses upon immunization with a mixture of VP11/12$_{129-143}$ and VP11/12$_{483-497}$ CD4$^+$ T cell epitopes against ocular herpes infection and disease. We demonstrated that induction of VP11/12$_{129-143}$ and VP11/12$_{483-497}$ epitope-specific CD4$^+$ T cells in the cornea correlated with protection. Based on these findings, in this article, we discuss our emerging concept of peripheral epithelial immunity and central neuronal immunity in the development of a forthcoming future T cell epitope-based herpes vaccine.

RESULTS

***In silico* prediction models and *in vitro* assays identify two VP11/12 CD4$^+$ T cell epitopes that bind with high affinity to the most common HLA-DR haplotypes.** We first identified 10 potential CD4$^+$ T cell epitopes within HSV-1 tegument protein VP11/12 (strain 17) using the TEPITOPE computer algorithm. The *in silico* TEPITOPE

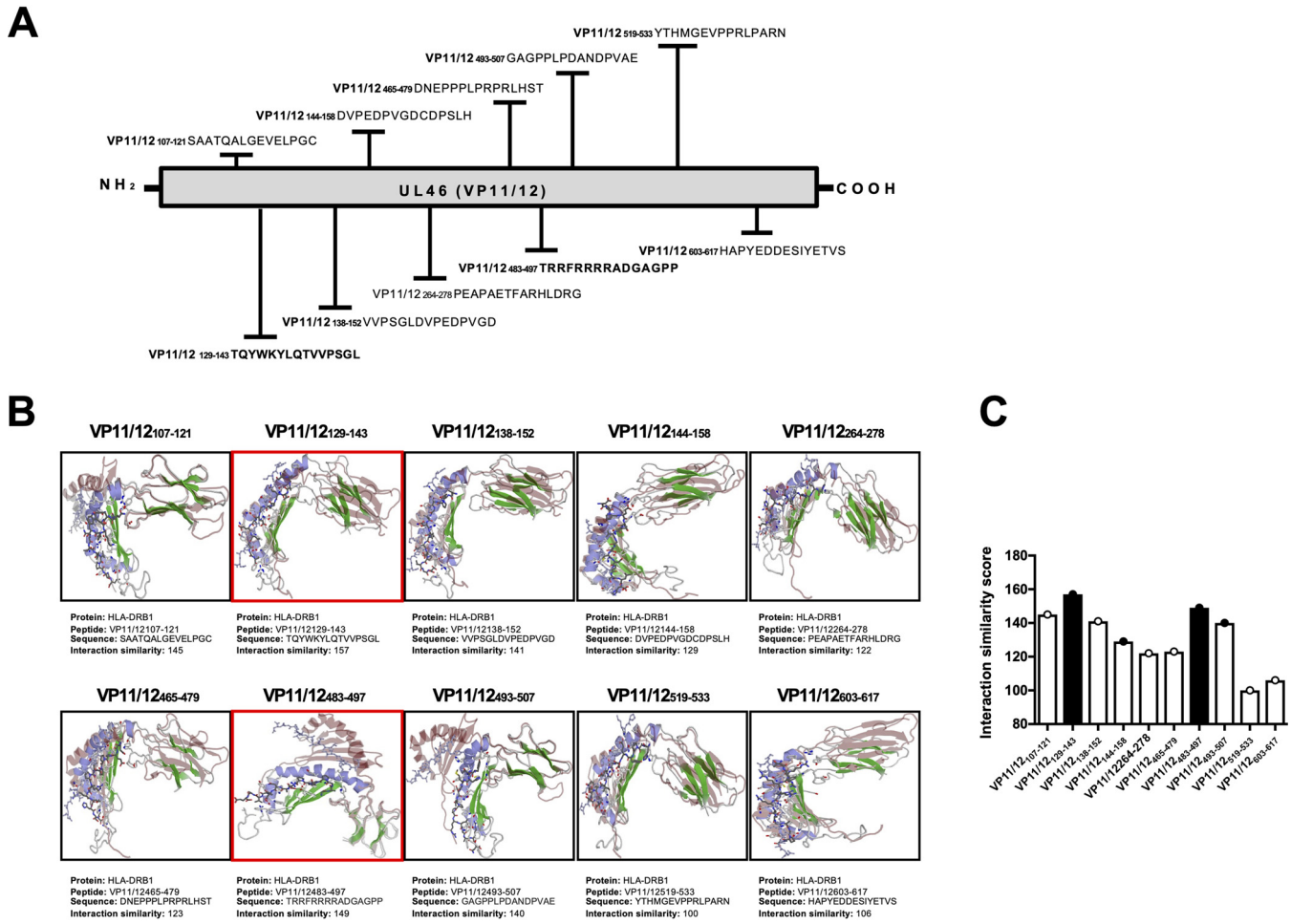

FIG 1 Illustrations of the relative locations of VP11/12 CD4$^+$ T cell epitopes and molecular docking for CD4$^+$ T cell epitope peptide–HLA-DRB1 molecule. (A) The sequence of the HSV-1 (strain 17) tegument protein (VP11/12) was submitted to the screening of potential HLA-DR epitopes using the TEPITOPE computer algorithm. Ten potential CD4$^+$ T cell epitopes were selected on the basis of high-affinity binding to multiple HLA-DR molecules. (B and C) Computational molecular docking of the 10 CD4$^+$ T cell peptide epitopes into the groove of the HLA-DRB1 protein (PDB accession no. 4GBX) was performed using the GalaxyPepDock server. The peptides are shown in ball and stick structures, and the HLA-DRB1 protein is shown as a template. The prediction accuracy is estimated from a linear model as the relationship between the fraction of correctly predicted binding site residues and the template-target similarity measured by the protein structure similarity score (TM score) and interaction similarity score (SInter) obtained by linear regression. SInter shows the similarity of the amino acids of the CD4$^+$ peptides aligned to the contacting residues in the amino acids of the HLA-DRB1 template structure. A higher SInter score represents a more significant binding affinity among the HLA-DRB1 molecule and CD4 peptides.

computational simulation-based prediction method predicts potential HLA-DRB1-restricted T cell epitopes. The amino acid sequence of HSV-1 VP11/12 tegument protein (strain 17) was screened for potential HLA-DRB1 binding regions, and the relative locations of 10 identified epitopes are illustrated in Fig. 1A.

We then performed peptide-protein docking analysis that evaluated the interaction between each of the 10 CD4 peptide epitopes and HLA-DRB1 molecules at the atomic level. This structural characterization method identifies candidate peptide epitopes with high binding affinity to HLA-DRB1 molecules. Molecular docking of 10 individual CD4 peptide epitopes into the DRB1 region of the binding protein identified by PDB accession number 4GBX (crystal structure of HLA-DM-HLA-DR1) was performed using the GalaxyPepDock server. The prediction accuracy was estimated from a linear model as the relationship between the fraction of correctly predicted binding site residues and the template-target similarity measured by the protein structure similarity score (TM score) and by the interaction similarity score (SInter) obtained by linear regression. SInter shows the similarity of the amino acids of the CD4 peptides aligned to the contacting residues in the amino acids of the HLA-DRB1 template. A relatively higher

TABLE 1 *In vitro* binding capacities of HSV-1 VP11/12-derived epitope peptides for soluble HLA-DR molecules

VP11/12 peptide (aa)	Relative activity by HLA-DR allele (serotype)[a]									
	DRB1*01:01 (DR1)	DRB1*03:01 (DR3)	DRB1*04:01 (DR4)	DRB1*07:01 (DR7)	DRB1*09:01 (DR9)	DRB1*11:01 (DR11)	DRB1*12:02 (DR12)	DRB1*13:01 (DR13)	DRB1*15:01 (DR15)	DRB1*15:02 (DR15)
107–121	>4,149	>119	>145	>336	>689	>278	>136	>263	>270	>3,333
129–143	**0.2**	>119	**0.1**	**0.1**	**6**	**1**	**17**	>263	163	**32**
138–152	>4,149	>119	>145	>336	>689	>278	>136	>263	>270	>3,333
144–158	>4,149	>119	>145	>336	>689	>278	>136	>263	>270	>3,333
264–278	>4,149	>119	>145	**93**	>689	256	>136	>263	>270	>3,333
465–479	>4,149	>119	>145	>336	>689	>278	>136	203	>270	>3,333
483–497	**61**	>119	>145	>336	>689	**9**	>136	>263	**46**	490
493–507	>4,149	>119	>145	>336	>689	>278	>136	>263	>270	>3,333
519–533	2,622	>119	>145	>336	>689	**6**	>136	>263	>270	>3,333
603–617	4,500	>119	>145	>336	>689	>278	>136	>263	>270	>3,333

[a]HSV-1 VP11/12-derived peptide epitopes were subjected to *in vitro* binding to soluble HLA-DRB1 molecules. Reference non-herpesvirus peptides were used to validate each assay. Data are expressed as relative activities (ratio of the IC_{50} of the peptide to the IC_{50} of the reference peptide) and are the means of two experiments. Peptide epitopes with high-affinity binding to HLA-DR molecules have IC_{50} values below 100 and are shown in bold. >, peptide epitope failed to bind to the tested HLA-DR molecule.

SInter score of 157 was observed for $VP11/12_{129-143}$, followed by an SInter score of 149 for $VP11/12_{483-497}$ (Fig. 1B and C). These higher SInter scores indicate strong binding affinity of $VP11/12_{129-143}$ and $VP11/12_{483-497}$ peptide epitopes to the HLA-DRB1 molecule.

To verify the strong predicted affinity of $VP11/12_{129-143}$ and $VP11/12_{483-497}$ peptide epitopes to the HLA-DRB1 molecules, we then determined *in vitro* binding to soluble HLA-DR molecules. Peptides corresponding to the 10 potential peptide epitopes, predicted above *in silico* with high affinity to HLA-DRB1 molecules, were synthetized and further tested *in vitro* for binding to 10 soluble HLA-DR molecules (Table 1). This panel of available HLA-DR molecules consists of the most common HLA class II haplotypes, regardless of ethnicity. The relative binding capacity (50% inhibitory concentration [IC_{50}], in nanomolars) for each peptide was calculated as the concentration of competitor peptide required to inhibit 50% of the binding of an allele-specific biotinylated peptide (indicator peptide), as described in Materials and Methods. Peptide epitopes with high-affinity binding to HLA-DR molecules have IC_{50} values below 100 nM. The peptides $VP11/12_{129-143}$ and $VP11/12_{483-497}$ bound to three or more different HLA-DR molecules, whereas the remaining peptides did not bind to even two or more HLA-DR molecules tested.

Altogether, the *in vitro* binding capacities of HSV-1 VP11/12-derived peptides for soluble HLA-DR molecules strengthen our *in silico* results of epitope prediction and molecular docking that predicted $VP11/12_{129-143}$ and $VP11/12_{483-497}$ as high-affinity binders of $CD4^+$ T cell epitopes to most common HLA-DRB1 molecules.

High frequency of $VP11/12_{129-143}$ and $VP11/12_{483-497}$ peptide-specific T cell responses in HSV-1-seropositive asymptomatic individuals. To verify the *in silico* prediction models and the *in vitro* binding results above, we next assessed the ability of synthetic peptides, corresponding to the 10 predicted $CD4^+$ T cell epitopes, to induce functional HSV-specific $CD4^+$ T cell responses in HSV-1-seropositive asymptomatic individuals. Specifically, the ability of each VP11/12 peptide to recall proliferative gamma interferon (IFN-γ)-producing $CD107^{a/b+}$ $CD4^+$ T cells was examined in 10 HSV-seropositive asymptomatic individuals.

$CD4^+$ T cells from HSV-seropositive asymptomatic individuals ($n = 10$) were stimulated with each of the 10 different VP11/12 peptides at a concentration of 10 μM in the presence of anti-CD28/49d, GolgiPlug, and GolgiStop for 6 h, and the frequency of IFN-γ-producing $CD4^+$ T cells was quantified using a fluorescence-activated cell sorter (FACS) assay. The highest frequencies of IFN-γ-producing $CD4^+$ T cell responses were detected against $VP_{129-143}$ (10.7%) and $VP11/12_{483-497}$ (8.6%) (Fig. 2A). The enzyme-linked immunosorbent spot assay (ELISpot) assay shown in Fig. 2B reveals the frequency distribution of IFN-γ-producing $CD4^+$ T cells induced by the 10 VP11/2 pep-

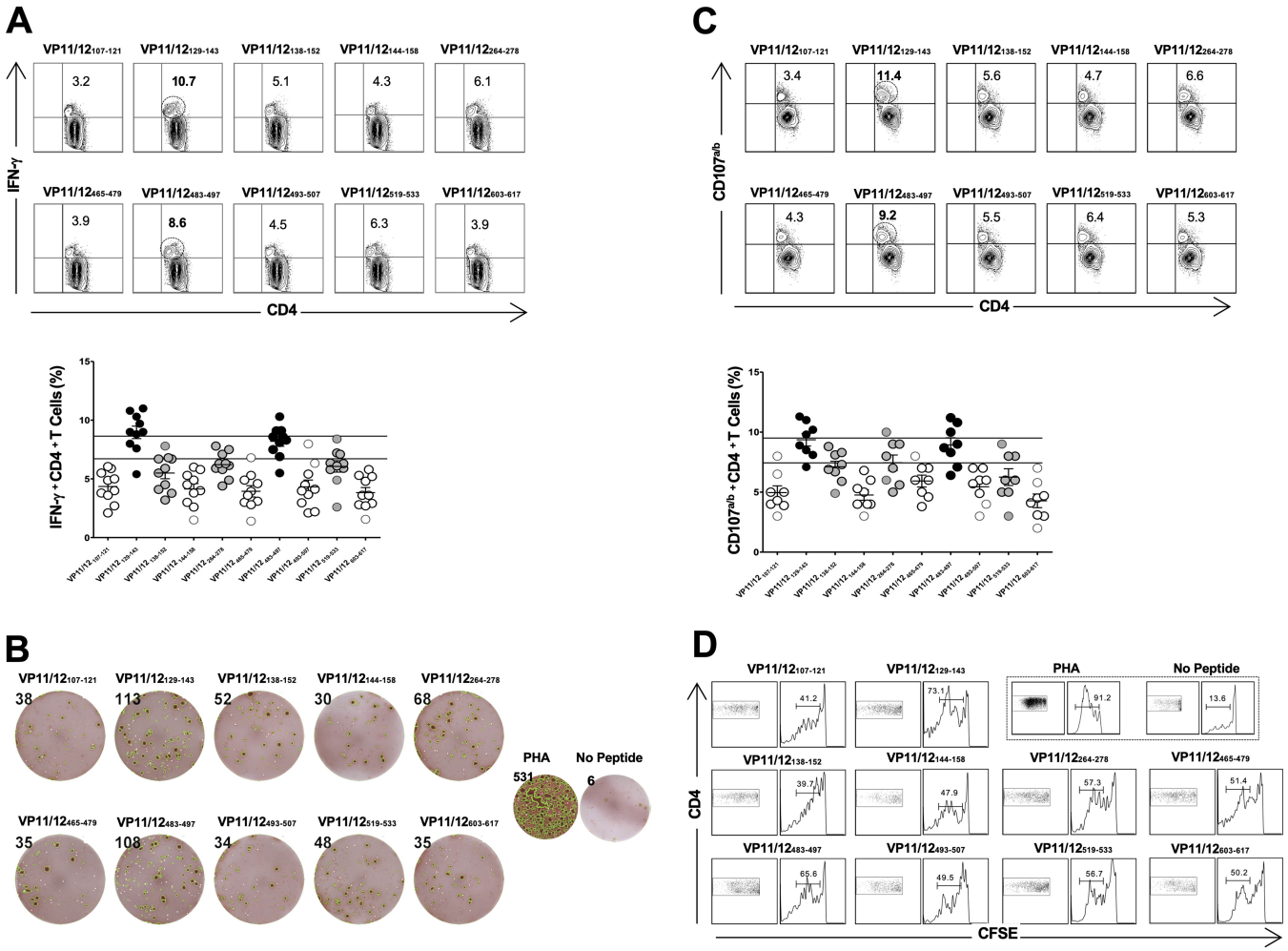

FIG 2 Prevalence of CD4$^+$ T cell responses specific to 10 VP11/12 epitopes in HSV-1-seropositive asymptomatic individuals. PBMCs from HSV-1-seropositive asymptomatic individuals ($n = 10$) were stimulated with 10 different VP11/12 peptides (10 μM) in the presence of anti-CD28/49d, anti-CD107a and -CD107b, GolgiPlug, and GolgiStop for 6 h. IFN-γ production and CD107$^{a/b}$ expression were then measured by FACS and ELISpot assay. (A) Representative FACS plot shows IFN-γ production by VP11/12 epitope-primed CD4$^+$ T cells (upper panel). The numbers on the top of each dot plot indicate the percentage of IFN-γ^+ CD4$^+$ T cells. The average frequencies of VP11/12 epitope-specific IFN-γ^+ CD4$^+$ T cells from 10 HSV-1-seropositive asymptomatic individuals are shown in the lower panel. (B) IFN-γ ELISpot assay of CD4$^+$ T cells from HSV-1-seropositive asymptomatic individuals following stimulation with 10 VP11/12 epitopes. Representative images of wells with IFN-γ-producing cells from PBMCs (0.5×10^6 cells/well) stimulated for 48 h with 10 μg of each VP11/12 peptide are depicted. The number on the top of each image represents the number of IFN-γ-producing spot-forming T cells per half a million total cells. PHA (1 μg/ml) and no peptide were used as positive and negative controls, respectively. (C) Representative FACS plots show the expression of CD107$^{a/b}$ from VP11/12 epitope peptide-primed CD4+ T cells. The numbers on the top of each dot plot indicate the percentage of CD107$^{a/b+}$ CD4$^+$ T cells (upper panels). Average percentages of VP11/12 epitope-specific CD107$^{a/b+}$ CD4$^+$ T cells from 10 HSV-seropositive asymptomatic individuals are shown in the lower panel. (D) Representative dot plots of the percentage of dividing CFSE$^+$ CD4$^+$ T cells from HSV-seropositive asymptomatic individuals following a six-day *in vitro* stimulation with each of the VP11/12 peptides. The results are representative of two experiments.

tides. Preliminary analysis of the IFN-γ-producing CD4$^+$ T cells revealed that 20 or more spots/10^6 CD4$^+$ T cells gave a 97% probability of defining a positive response. Based on the number of IFN-γ-producing CD4$^+$ T cells, the response was ranked as follows: strong responses, >80 spot-forming cells (SFC) per half million peripheral blood mononuclear cells (PBMCs) (SFCs/0.5×10^6); medium responses, >40 and <80 SFCs; low responses, >20 and <40 SFCs. Similar to intracellular staining, the ELISpot assay confirmed that the highest IFN-γ-producing CD4$^+$ T cell responses were directed to the $VP_{129-143}$ (113 spots) and $VP11/12_{483-497}$ (108 spots) epitopes (Fig. 2B). In contrast, a medium frequency of IFN-γ-producing CD4$^+$ T cell responses was detected against $VP11/12_{138-152}$ (52 spots), $VP11/12_{264-278}$ (68 spots), and $VP11/12_{519-533}$ (48 spots), while the lowest numbers of SFCs were detected against the remaining five VP11/12 peptides. As expected, all of the donors responded similarly to phytohemagglutinin (PHA;

positive control) while no SFCs were recorded in the absence of stimulating peptides (negative controls).

Furthermore, we tested whether VP11/12 CD4 peptides display any cytotoxic activity by performing a CD107$^{a/b}$ degranulation assay *ex vivo* on freshly isolated PBMCs. As shown in Fig. 2C, of the 10 VP11/12 peptide epitopes, VP11/12$_{129-143}$ (11.4%) and VP11/12$_{483-497}$ (9.2%) induced the most significant degranulation/mobilization of CD107$^{a/b}$ on the surface of CD4$^+$ T cells from HSV-1-seropositive individuals. Since a lack of IFN-γ production and CD107$^{a/b}$ expression may not always reflect the lack of a T cell response, we also studied the proliferative response of CD4$^+$ T cells to the 10 VP11/12 peptides from HSV-1-seropositive asymptomatic individuals. PBMCs were labeled with carboxyfluorescein succinimidyl ester (CFSE) and then stimulated *in vitro* for 6 days with each of the 10 VP11/12 CD4$^+$ peptides. VP11/12$_{129-143}$ and VP11/12$_{483-497}$ induced the highest proliferation of CD4$^+$ T cells (Fig. 2D).

Altogether, these functional results (i) confirm the *in silico* prediction and the *in vitro* binding results described above and (ii) suggest that VP11/12$_{129-143}$ and VP11/12$_{483-497}$ are immunodominant CD4$^+$ T cell epitopes.

Human CD4$^+$ T cells specific to VP11/12$_{129-143}$ and VP11/12$_{483-497}$ epitopes are of the T$_{EM}$ phenotype and recognize native epitopes naturally processed and presented by HSV-1-infected cells. Conventional circulating HSV-specific memory CD4$^+$ T cells are categorized into two major phenotypically and functionally distinct subsets: the effector memory (T$_{EM}$) and the central memory (T$_{CM}$) cell subsets. We next investigated the phenotype and function of asymptomatic human CD4$^+$ T cells specific to the VP11/12$_{129-143}$ and VP11/12$_{483-497}$ epitopes. CD4$^+$ T cell lines specific to each of the two HSV-1 VP11/12 epitopes were generated. As shown in Fig. 3A, the vast majority of the CD4$^+$ T cell lines specific to VP11/12$_{129-143}$ (82.3%) and VP11/12$_{483-497}$ (68.9%) are of a CD44^{high} CC62L^{low} CD4$^+$ T$_{EM}$ phenotype. These findings suggest that most of VP11/12$_{129-143}$ and VP11/12$_{483-497}$ epitope-specific CD4$^+$ T cells from naturally protected HSV-1-seropositive asymptomatic individuals are of the T$_{EM}$ phenotype.

Because these CD4$^+$ T cells specific to VP11/12$_{129-143}$ and VP11/12$_{483-497}$ epitopes were generated *in vitro* using artificial synthetic peptides, it was of interest to determine whether they recognized native viral epitopes that are naturally processed and presented by HSV-1-infected target cells. Therefore, we analyzed the ability of HLA-DR-positive HSV-1-infected target dendritic cells (DCs) (antigen-presenting dendritic cells [APCs]) to process and present native epitopes that would be recognized by the autologous VP11/12$_{129-143}$ and VP11/12$_{483-497}$ epitope-specific CD4$^+$ T cell lines. CD4$^+$ T cells specific to VP11/12$_{129-143}$ and VP11/12$_{483-497}$ peptides underwent significant IFN-γ production (Fig. 3B and D) and CD107$^{a/b}$ degranulation (Fig. 3C) when incubated with autologous HLA-DR-positive DC infected with HSV-1 ($P < 0.05$). Moreover, expression of both the CD69 and CD44 activation markers was induced on the VP11/12$_{129-143}$ and VP11/12$_{483-497}$ CD4$^+$ T cell lines when they were incubated with HLA-DR-positive autologous DC infected with HSV-1 ($P < 0.05$) (Fig. 3E and F). As expected, significant functions were detected when target DC were pulsed with a test peptide epitope (VP11/12$_{129-143}$ or VP11/12$_{483-497}$). In contrast, no functional activities were detected in the VP11/12$_{129-143}$ and VP11/12$_{483-497}$ CD4$^+$ T cell lines when incubated with autologous target DC pulsed with a control peptide (VP11/12$_{107-121}$), indicating the epitope specificity of the responses. Altogether, these results demonstrate that the human CD4$^+$ T cells specific to the VP11/12$_{129-143}$ and VP11/12$_{483-497}$ epitopes (i) were of effector memory phenotype (T$_{EM}$) and (ii) recognized native epitopes naturally processed and presented by HSV-1-infected cells.

Three VP11/12 regions that contain immunodominant CD4$^+$ T cell epitopes are identified using the PepScan library mapping strategy. To determine whether there were other potential VP11/12 CD4$^+$ T epitopes, in addition to the VP11/12$_{129-143}$ and VP11/12$_{483-497}$ epitopes identified above, we used the PepScan library as an alternative mapping strategy; using this approach, 89 peptides were synthesized with 15-aa overlapping sequences, as illustrated in Fig. 4. This PepScan library of peptides was

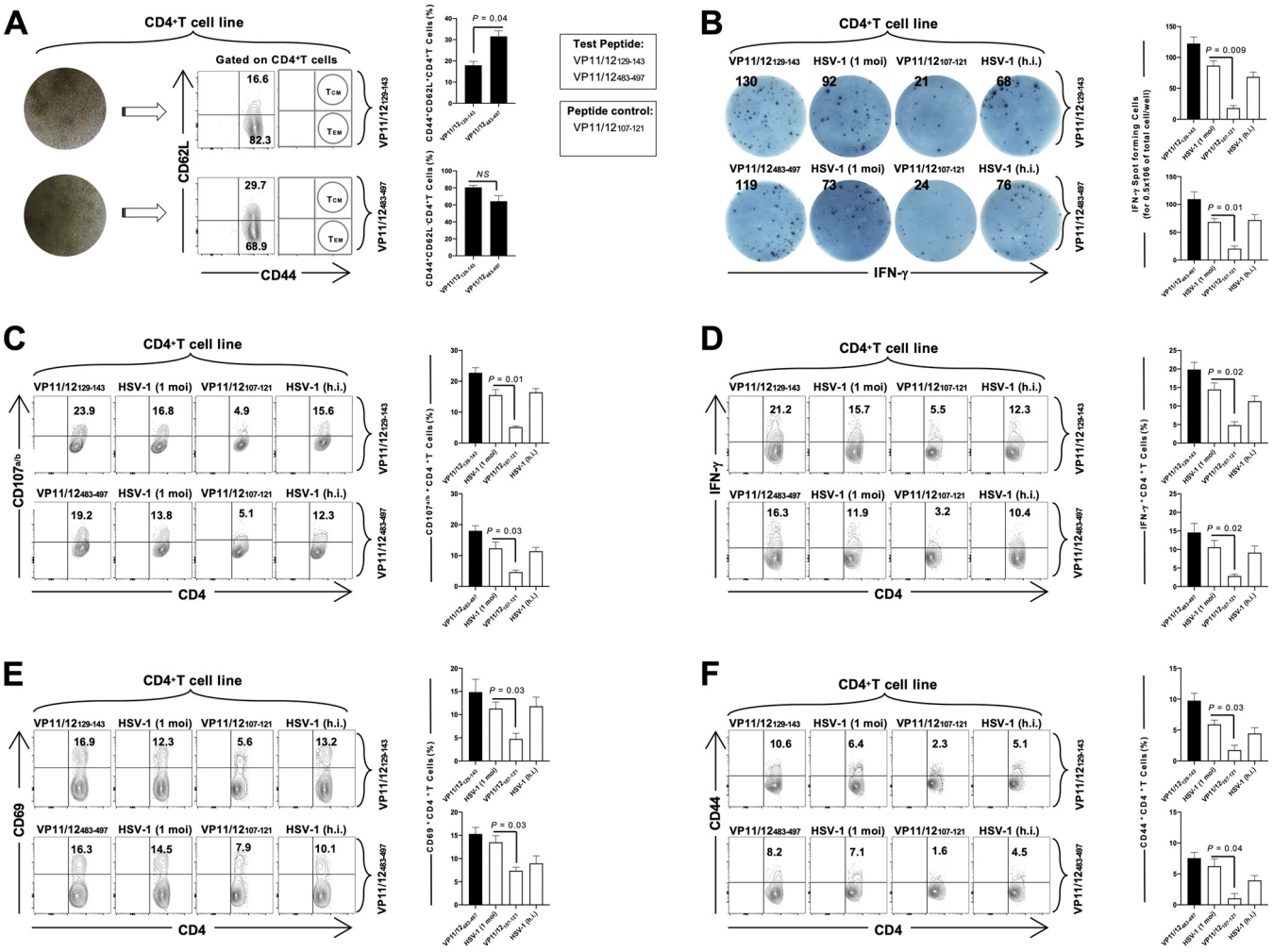

FIG 3 Phenotypic and functional characterization of CD4+ T_{EM} cell lines specific to the immunodominant VP11/12$_{129-143}$ and VP11/12$_{483-497}$ epitopes. VP11/12$_{129-143}$ and VP11/12$_{483-497}$ peptide-specific CD4+ T cell lines were generated from HLA-DR-positive and HSV-1-seropositive asymptomatic individuals, and their T_{EM} and T_{CM} phenotype and function were analyzed. (A) FACS data show representative average frequencies (left panels) of CD44^{high} CD62L^{low} CD4+ T_{EM} cells and (right panels) CD44^{high} CD62L^{high} CD4+ T_{CM} cells specific to VP11/12$_{129-143}$ and VP11/12$_{483-497}$ epitopes. (B) ELISpot results show representative (left) and average (right) frequencies of IFN-γ-producing CD4+ T_{EM} cells following stimulation with autologous DC pulsed with test peptides (VP11/12$_{129-143}$ or VP11/12$_{483-497}$) or control peptide (VP11/12$_{107-121}$) or infected with HSV-1 (native epitopes). The number on the top of each image represents the number of IFN-γ-producing spot-forming T cells per half a million total cells. (C to F) Representative (left) and average (right) frequencies of CD107$^{a/b+}$ CD4+ T_{EM} cells (C), IFN-γ-producing CD4+ T_{EM} cells (D), CD69+ CD4+ T_{EM} cells (E), and CD44+ CD4+ T_{EM} cells (F) following stimulation with autologous DC pulsed with test peptides (VP11/12$_{129-143}$ or a VP11/12$_{483-497}$) or control peptide (VP11/12$_{107-121}$) or infected with HSV-1 (native epitopes). The results are representative of three experiments.

divided into nine distinct pools of peptides with 10 individual overlapping peptides forming each pool.

We next assessed the ability of the nine pools of peptides to induce functional HSV-specific CD4+ T cell responses in HSV-1-seropositive asymptomatic individuals. PBMCs from 10 HSV-seropositive asymptomatic individuals were stimulated with the nine different pools of VP11/12 peptides in the presence of anti-CD28/49d, GolgiPlug, and GolgiStop for 6 h. The highest frequency of IFN-γ-producing CD4+ T cells was detected from HSV-seropositive asymptomatic individuals against pool 2 (8.3%) and pool 5 (7.6%) (Fig. 5A). In contrast, a medium frequency of IFN-γ-producing CD4+ T cells was detected against pool 7 (4.9%) (Fig. 5A). Moreover, pool 2 (8.9%) and pool 5 (7.4%) induced a significantly higher frequency of CD107$^{a/b+}$ CD4+ T cells (Fig. 5B). Similarly, significantly higher IFN-γ-producing CD4+ T cell responses were detected by the ELISpot assay for pool 2 (86 spots) and pool 5 (78 spots), while a medium frequency was detected in pool 7 (44 spots) (Fig. 5C). Lower frequencies of IFN-γ+ CD4+ T cells and CD107$^{a/b+}$ CD4+ T cells were detected in pool 1, pool 3, pool 4, pool 6, pool 8, and

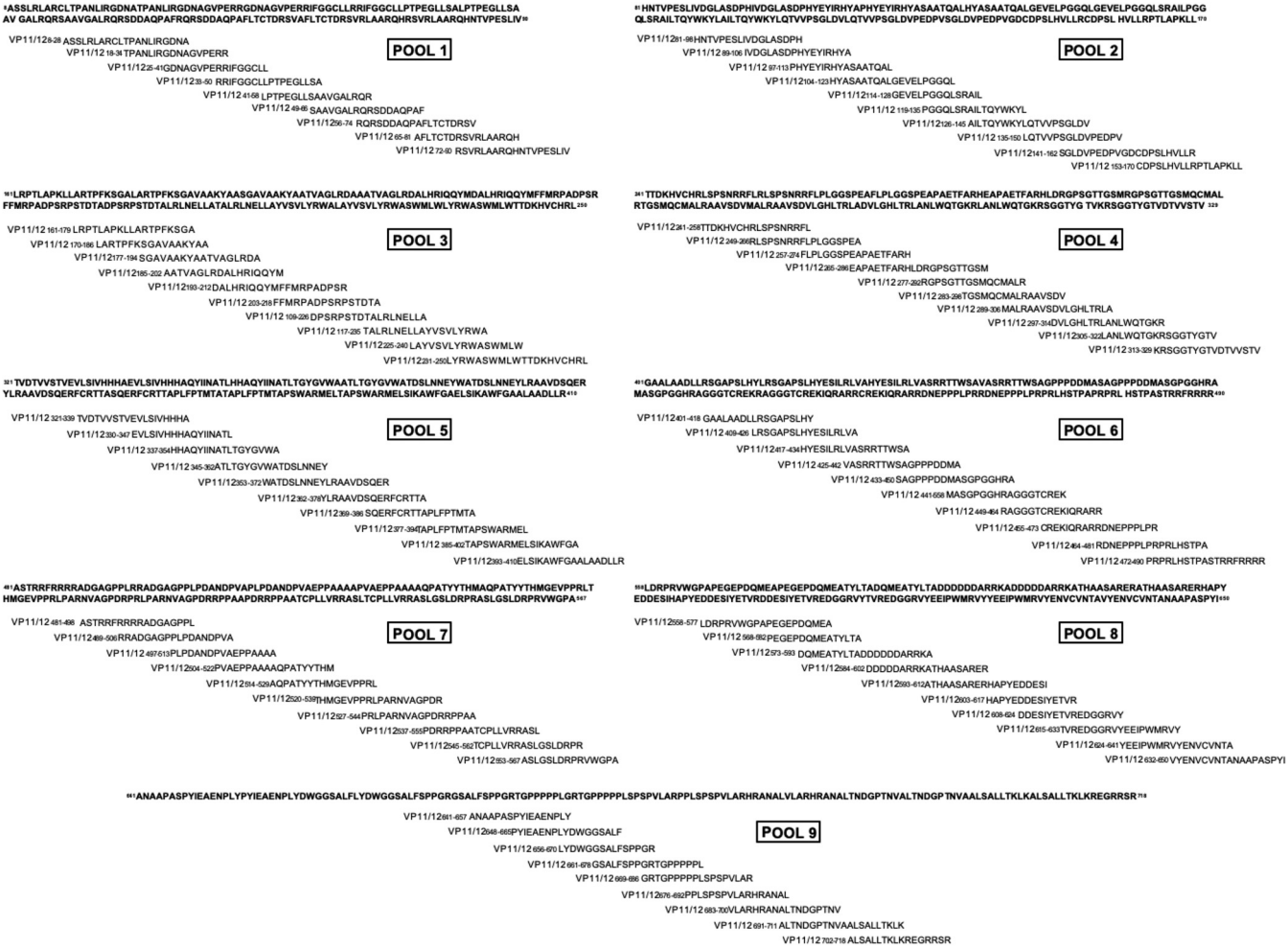

FIG 4 The PepScan library of peptides was designed from the HSV-1 tegument protein (VP11/12) sequence consisting of 716 aa (strain 17; NCBI accession number P10230). Shown are the sequences of nine pools of overlapping peptides (pool 1 to pool 9). Each pool contains 10 overlapping 15- to 21-mer VP11/12 peptides.

pool 9. As expected, all the asymptomatic individuals responded similarly to PHA (positive control). Altogether, these results indicate that three VP11/12 regions, representing peptides from pool 2, pool 5, or pool 7, contain one or several immunodominant CD4$^+$ T cell epitopes.

The immunodominant VP11/12$_{129-143}$ and VP11/12$_{483-497}$ CD4$^+$ T cell epitopes confirmed using the PepScan library mapping strategy. We next evaluated the ability of the 10 individual peptides forming each PepScan library mapping immunodominant pool 2, pool 5, and pool 7 to induce HSV-specific CD4$^+$ T cell responses in 10 HSV-seropositive asymptomatic individuals. As shown in the representative FACS plots in Fig. 6A and average frequencies in Fig. 6C, the highest frequencies of IFN-γ^+ CD4$^+$ T cells were directed against four different peptide epitopes from pool 2: VP11/12$_{89-106}$ (5.1%), VP11/12$_{104-123}$ (4.2%), VP11/12$_{126-145}$ (8.5%), and VP11/12$_{135-150}$ (6.8%). Similarly, the highest frequency of IFN-γ^+ CD4$^+$ T cells was directed against two peptide epitopes from pool 5 and pool 7: VP11/12$_{345-362}$ (5.6%) and VP11/12$_{353-372}$ (8.9%) from pool 5 and VP11/12$_{481-498}$ (8.1%) and VP11/12$_{489-506}$ (4.5%) from pool 7. The sequences of the VP11/12$_{126-145}$ and VP11/12$_{481-498}$ epitopes identified using the PepScan library mapping strategy overlap the sequences of the two immunodominant VP11/12$_{129-143}$ and VP11/12$_{481-498}$ epitopes identified using the TEPITOPE mapping strategy described above.

Furthermore, as shown in the representative FACS plots in Fig. 6B and average frequencies in Fig. 6D, the highest frequencies of CD107$^{a/b+}$ CD4$^+$ T cells were directed

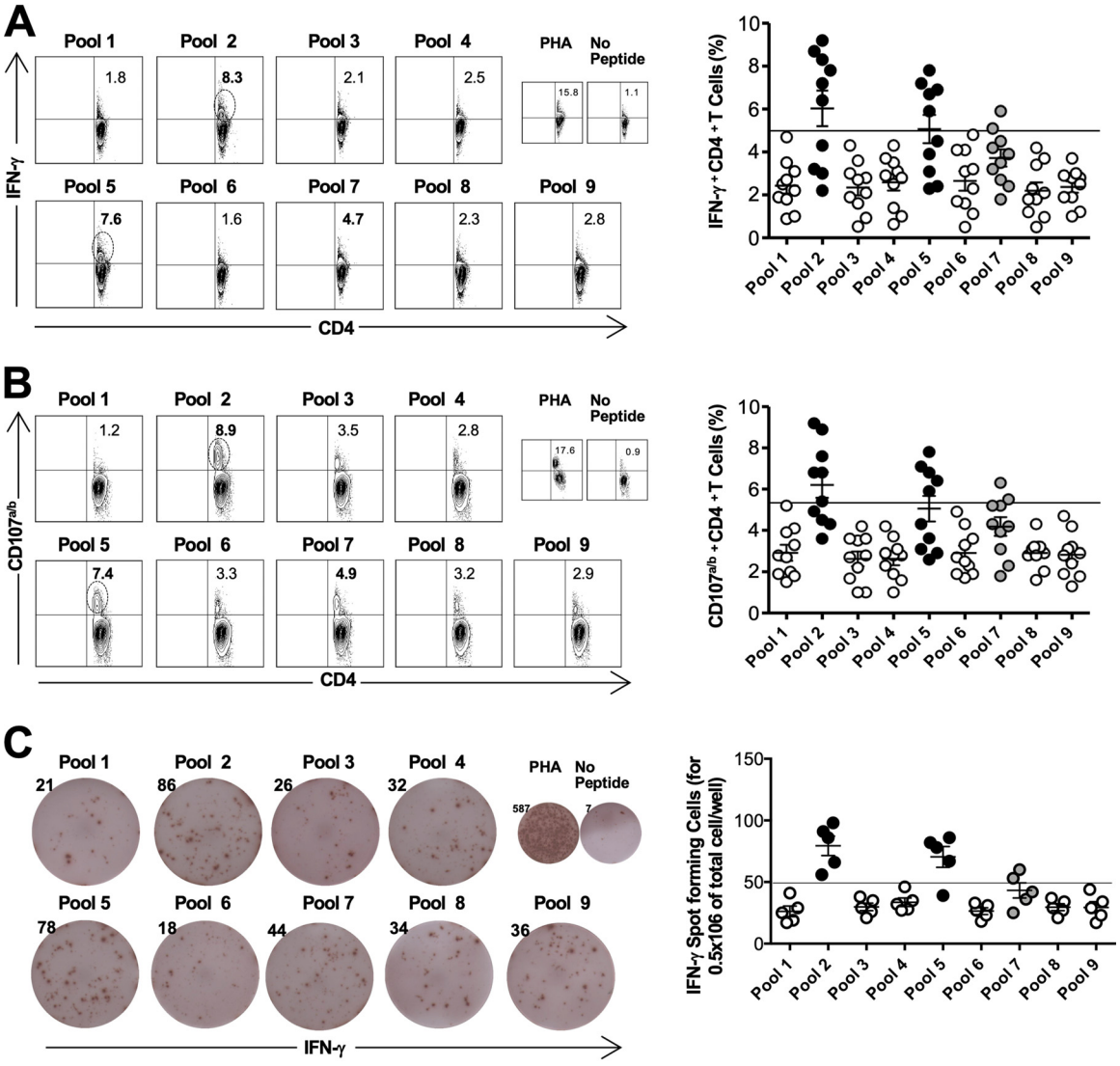

FIG 5 IFN-γ production and CD107$^{a/b}$ expression by HSV-specific CD4$^+$ T cells following stimulation with nine pools of VP11/12 peptides. PBMCs from HSV-seropositive asymptomatic individuals were stimulated with 9 separate pools of VP11/12 peptides. Each pool contains 10 VP11/12 overlapping peptides. (A) Representative FACS plots (left) and average percentages (right) of IFN-γ-producing CD4$^+$ T cells stimulated with 9 pools of VP11/12 peptides. The numbers on the top of each dot plot indicate the percentages of IFN-γ^+ CD4$^+$ T cells. (B) Representative FACS plots (left) and average percentages (right) of CD107$^{a/b}$ CD4$^+$ T cells stimulated with 9 pools of VP11/12 peptides. The numbers on the top of each dot plot indicate the percentages of CD107$^{a/b}$ CD4$^+$ T cells. (C) The 9 pools of VP11/12 peptides were analyzed through ELISpot assay for their capacity to elicit IFN-γ production (left). The numbers on the top of each image of representative ELISpot wells indicate the numbers of IFN-γ-producing spot-forming T cells per half a million total cells. Data are the average of IFN-γ-producing cells measured by ELISpot assay from five asymptomatic individuals (right). PHA (1 μg/ml) and no peptide used as positive and negative controls, respectively. The results are representative of two experiments.

against four different peptide epitopes from pool 2: VP11/12$_{89-106}$ (4.9%), VP11/12$_{104-123}$ (4.1%), VP11/12$_{126-145}$ (7.7%), and VP11/12$_{135-150}$ (5.4%). Similarly, the highest frequencies of IFN-γ^+ CD4$^+$ T cells were directed against two peptide epitopes from pool 5 and pool 7: VP11/12$_{345-362}$ (4.1%) and VP11/12$_{353-372}$ (8.1%) from pool 5 and VP11/12$_{481-498}$ (7.2%) and VP11/12$_{489-506}$ (3.9%) from pool 7.

Altogether, these results demonstrate that IFN-γ-producing CD4$^+$ T cells expressing cytotoxic CD107$^{a/b}$ markers detected from HSV-1-seropositive asymptomatic individuals were directed against eight individual peptide epitopes derived from the whole VP11/12 protein: VP11/12$_{89-106}$, VP11/12$_{104-123}$, VP11/12$_{126-145}$, VP11/12$_{135-150}$, VP11/12$_{345-362}$, VP11/12$_{353-372}$, VP11/12$_{481-498}$, and VP11/12$_{489-506}$. In addition, the immunodominant VP11/12$_{129-143}$ and VP11/12$_{483-497}$ CD4$^+$ T cell epitopes identified above

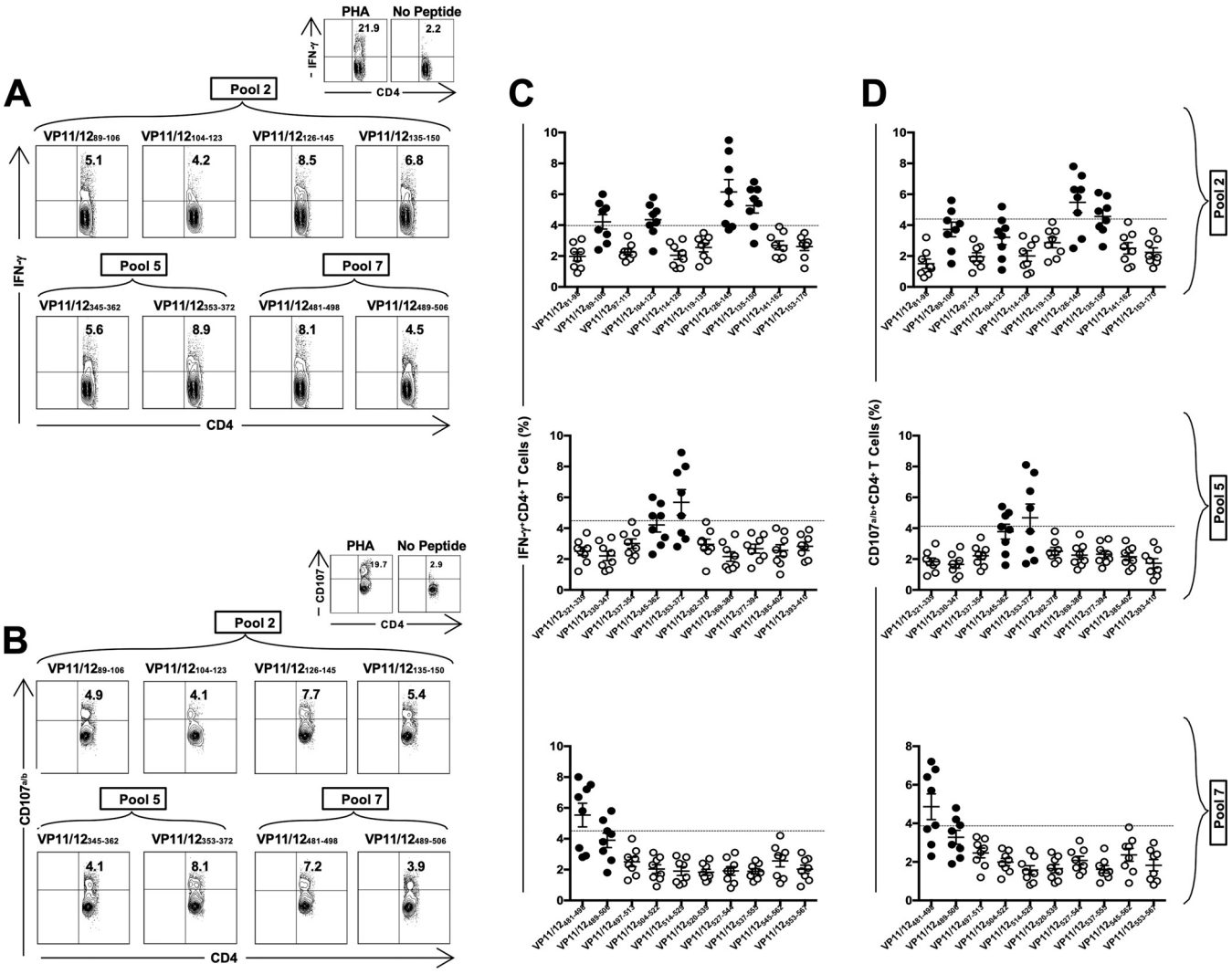

FIG 6 IFN-γ production and CD107$^{a/b}$ expression by HSV-specific CD4$^+$ T cells following stimulation with individual peptides from the dominant pools, as indicated. PBMCs from 10 HSV-seropositive asymptomatic individuals were stimulated *in vitro* with individual CD4$^+$ T cell peptide epitopes derived from the indicated pools of HSV-1 VP11/12 protein (a total of 30 peptides at 10 μM each). Peptide simulation was performed in the presence of anti-CD28/49d, anti-CD107^a and -CD107^b, GolgiPlug, and GolgiStop for 6 h. IFN-γ production and CD107$^{a/b}$ expression were then measured by FACS. (A and B) Representative FACS plots showing the percentages of IFN-γ$^+$ CD4$^+$ T (A) and CD107$^{a/b+}$ CD4$^+$ T cells (B) detected from the immunodominant peptides from pools 2, 5, and 7. (C and D) Average frequencies of IFN-γ$^+$ CD4$^+$ T cells (C) and CD107$^{a/b+}$ CD4$^+$ T cells (D) detected in 10 HSV-seropositive asymptomatic individuals. The results are representative of two experiments.

were confirmed using the PepScan library mapping strategy. Moreover, the sequences of the VP11/12$_{129-143}$ and VP11/12$_{483-497}$ epitopes are highly conserved between HSV-1 (95 to 100%) strains (Table 2).

The immunodominant VP11/12$_{129-143}$ and VP11/12$_{483-497}$ epitopes specific to effector CD4$^+$ T$_{EM}$ cells are less targeted by FOXP3$^+$ CD4$^+$ CD25$^+$ regulatory T cells. Furthermore, high frequencies of proliferative CD4$^+$ T cells were induced in the majority of HSV-1-seropositive asymptomatic individuals by three peptide epitopes: VP11/12$_{126-145}$ (up to 11.4%), VP11/12$_{353-372}$ (up to 12.1%), and VP11/12$_{481-498}$ (up to 9.1%) (Fig. 7A). The effector CD4$^+$ T cells specific to these three peptides produced IFN-γ, as confirmed by the ELISpot assay (Fig. 7B). High frequencies of IFN-γ-producing CD4$^+$ T cells were detected for VP11/12$_{126-145}$ (133 spots), VP11/12$_{135-150}$ (90 spots), VP11/12$_{353-372}$ (123 spots), and VP11/12$_{481-498}$ (100 spots), while medium frequencies of IFN-γ-producing CD4$^+$ T cells were detected against VP11/12$_{89-106}$ (69 spots), VP11/12$_{104-123}$ (43 spots), VP11/12$_{345-362}$ (61 spots), and VP11/12$_{489-506}$ (42 spots). In contrast, the immunodominant VP11/12 epitopes were not targeted by FOXP3$^+$ CD4$^+$

TABLE 2 Overlapping sequences of HSV-1 VP11/12 CD4$^+$ T cell epitopes between the HSV-1 and HSV-2 strains

Virus and strain (accession no.)	Sequence of the indicated VP11/12 epitope (aa)[a]		
	129–143	264-278	483–497
HSV-1			
17 (NC_001806.2)	TQYWKYLQTVVPSGL	PEAPAETFARHLDRG	TRRFRRRRADGAGPP
McKrae (JX142173.1)	TQYWKYLQTVVPSGL	PEAPAETFARHLDRG	TRRFRRRRADGAGPP
KOS (JQ673480.1)	TQYWKYLQTVVPSGL	PEAPAETFARHLDRG	TRRFRRRRADGAGPP
F (GU734771.1)	TQYWKYLQTVVPSGL	PEAPAETFARHLDRG	TRRFRRRRADGAAPP
RE (KF498959.1)	TQYWKYLQTVVPSGL	PEAPAETFARHLDRG	**A**RRFRRRRADGAGPP
HSV-2			
SHG52 (NC_001798.2)	**A**QYWKYLQTVVPSGL	**L**EAPAETFARHLDRG	**VDAADRGPEPC**AG**R**P
186 (JX112656.1)	**A**QYWKYLQTVVPSGL	**L**EAPAETFARHLDRG	**HVDAADR**GPEPCAGR

[a]The amino acid residues that are conserved across different HSV-1 and HSV-2 strains are shown in bold. The nonidentical amino acids between HSV-1 and HSV-2 herpesviruses are underlined.

CD25$^+$ regulatory T (T_{reg}) cells from HSV-seropositive asymptomatic individuals (Fig. 7C). Low frequencies of FOXP3$^+$ CD4$^+$ CD25$^+$ T_{reg} cells were detected against the immunodominant VP11/12 epitopes VP11/12$_{126–145}$ (3.2%) and VP11/12$_{353–372}$ (3.6%). However, medium frequencies of FOXP3$^+$ CD4$^+$ CD25$^+$ T_{reg} cells were detected against the subdominant epitopes VP11/12$_{481–498}$ (5.3%) and VP11/12$_{489–506}$ (6.2%) (Fig. 7C).

Altogether, these results(i) demonstrated that VP11/12$_{126–145}$, VP11/12$_{353–372}$, VP11/12$_{481–498}$, and VP11/12$_{489–506}$ peptide epitopes were major targets by multifunctional effector CD4$^+$ T cells but were less targeted by FOXP3$^+$ CD4$^+$ CD25$^+$ T_{reg} cells and (ii) confirmed that VP11/12$_{129–143}$ and VP11/12$_{483–497}$ are immunodominant effector CD4$^+$ T cell epitopes.

Protective immunity against ocular herpes virus infection and disease induced by the immunodominant VP11/12$_{129–143}$ and VP11/12$_{483–497}$ CD4$^+$ T cell epitopes in HLA-DR mice. Finally, we set up a preclinical vaccine trial using our established HLA-DR transgenic mouse model of ocular herpes to evaluate whether immunization with the immunodominant VP11/12$_{129–143}$ and VP11/12$_{483–497}$ CD4$^+$ T cell epitopes would confer protection against ocular herpes virus infection and disease. The protective efficacy of the two immunodominant epitopes was compared side by side with that induced by subdominant VP11/12$_{107–121}$ and VP11/12$_{603–617}$ epitopes. Three groups of HLA-DR transgenic mice ($n = 10$ mice/group) were immunized subcutaneously (s.c.) twice, at 21-day intervals, with either a mixture of immunodominant peptide epitopes (VP11/12$_{129–143}$ and VP11/12$_{483–497}$) or with a mixture of subdominant peptide epitopes (VP11/12$_{107–121}$ and VP11/12$_{603–617}$) emulsified in CpG$_{1826}$ adjuvant (100 μg of each peptide plus 2 μg of CpG$_{1826}$). The CpG$_{1826}$ adjuvant alone was used as a control (mock vaccination).

Two weeks after the second and final immunization, animals from all groups received an ocular HSV-1 challenge (2×10^5 PFU of strain McKrae) without scarification. The mice were then assessed for up to 30 days postchallenge for ocular herpes pathology, ocular viral titers, and survival, as illustrated in Fig. 8A. On day 7 postinfection, the clinical scores of corneal diseases observed in the mice immunized with the two immunodominant peptide epitopes were significantly lower than clinical scores observed in mice immunized with the two subdominant peptide epitopes and than those of the mock-immunized group ($P = 0.02$) (Fig. 8B). Furthermore, a significantly lower virus titer was detected on day 7 postinfection (the peak of viral replication) in the eye swabs of the immunodominant group than in the mock-immunized group ($P = 0.03$) (Fig. 8C). Most animals in the immunodominant group survived infection (75%) whereas survival was 50% in the subdominant group and only 35% in the mock-immunized group ($P = 0.03$) (Fig. 8D). Representative images in Fig. 8E show lower ocular disease observed in HLA-DR transgenic mice immunized with immunodominant peptides than in those immunized with subdominant peptides and mock immunized. Moreover, significantly higher frequencies of IFN-γ-producing CD4$^+$ T cells

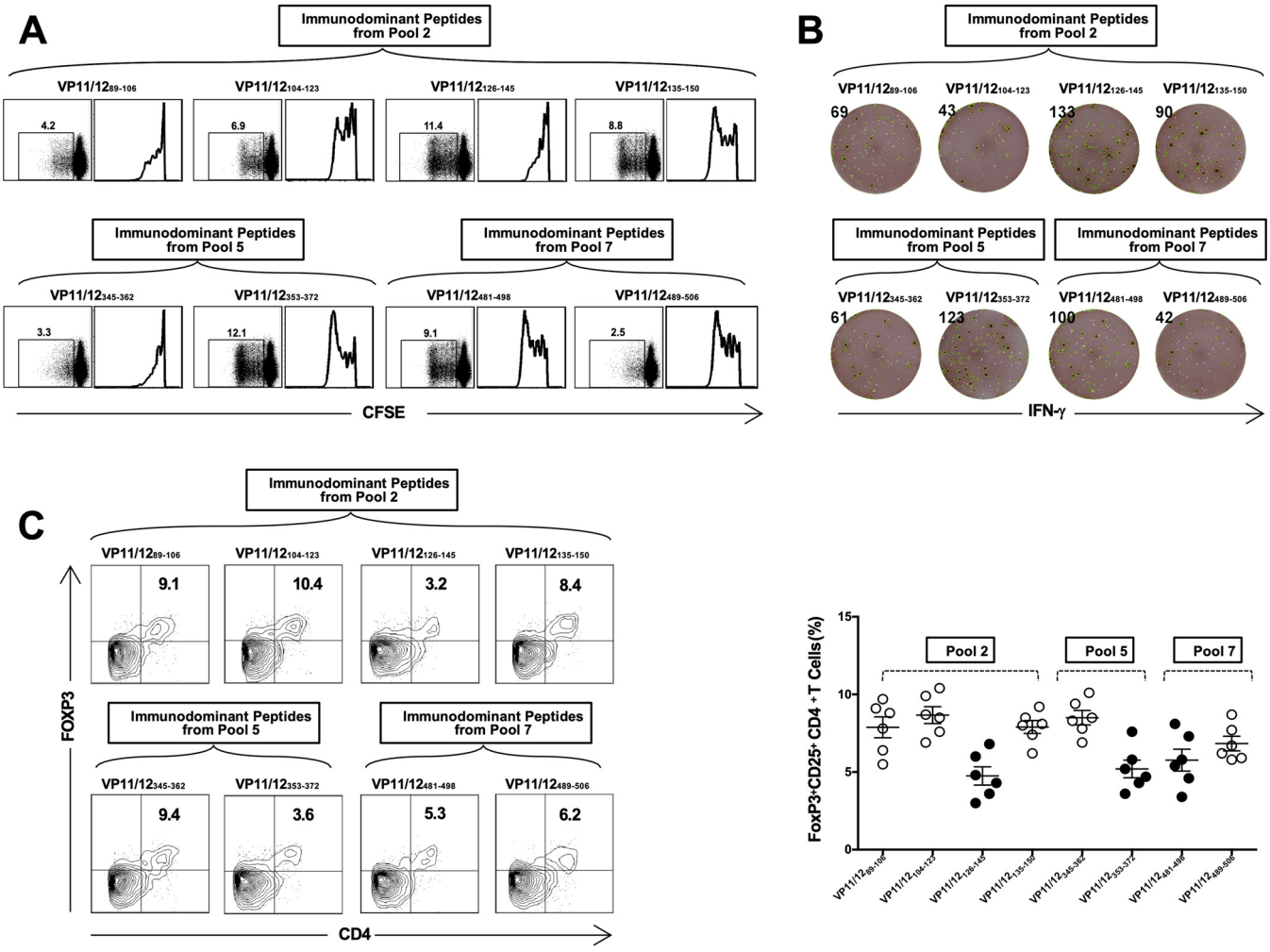

FIG 7 CFSE incorporation and frequency of regulatory cells in HSV-specific CD4$^+$ T cells following stimulation with individual peptides from the dominant pools, as indicated. PBMCs were stained with carboxyfluorescein succinimidyl ester (CFSE) (2 mM) and then stimulated for 6 days with the immunodominant individual VP11/12 peptides selected from pools 2, 5, and 7. A total of eight peptides (four peptides from pool 2, two peptides from pool 5, and 2 peptides from pool 7 at 10 μM each). (A) Representative dot plots and histograms showing the percentages and intensity of dividing CFSE$^+$ CD4$^+$ T cells from HSV-seropositive asymptomatic individuals following in vitro stimulation with eight immunodominant VP11/12 peptides. (B) Immunodominant peptides from VP11/12 peptide pools were analyzed through ELISpot assay for their capacity to elicit IFN-γ production (right). The number on the top of each image of representative ELISpot wells indicates the number of IFN-γ-producing spot forming T cells per half a million total cells. (C) PBMCs were stimulated with eight individual VP11/12 peptides and then stained for CD4, CD25, and Foxp3 expression on gated CD25^{high} and CD4$^+$ T cells. Representative FACS plots (left) and average frequencies (right) of Foxp3$^+$ CD4$^+$ T cells specific to each of the immunodominant VP11/12 peptides detected in 10 HSV-1-seropositive asymptomatic individuals are shown. Data are representative of two independent experiments.

were detected in the cornea of in HLA-DR transgenic mice immunized with the mixture of the two immunodominant epitopes (10.5%) than in those immunized with subdominant epitopes (4.3%) or mock immunized (2.4%) ($P = 0.03$) (Fig. 8F). Similarly, the highest frequencies of CD107$^{a/b}$-expressing CD4$^+$ T cells were mainly detected in the immunodominant group (15.7%) than in the subdominant group (7.6%) or mock group (5.4%) ($P = 0.02$) (Fig. 8G).

Altogether, these *in vivo* results (i) confirm that the immunodominant VP11/12$_{129-143}$ and VP11/12$_{483-497}$ CD4$^+$ T cell epitopes are targeted by protective T cells and (ii) demonstrate that immunization with the two immunodominant epitopes decreased ocular herpes infection and disease.

DISCUSSION

Evidence in both animal models and humans indicates that CD4$^+$ T cell-mediated protective immunity is, directly or indirectly, related to the control of HSV infection

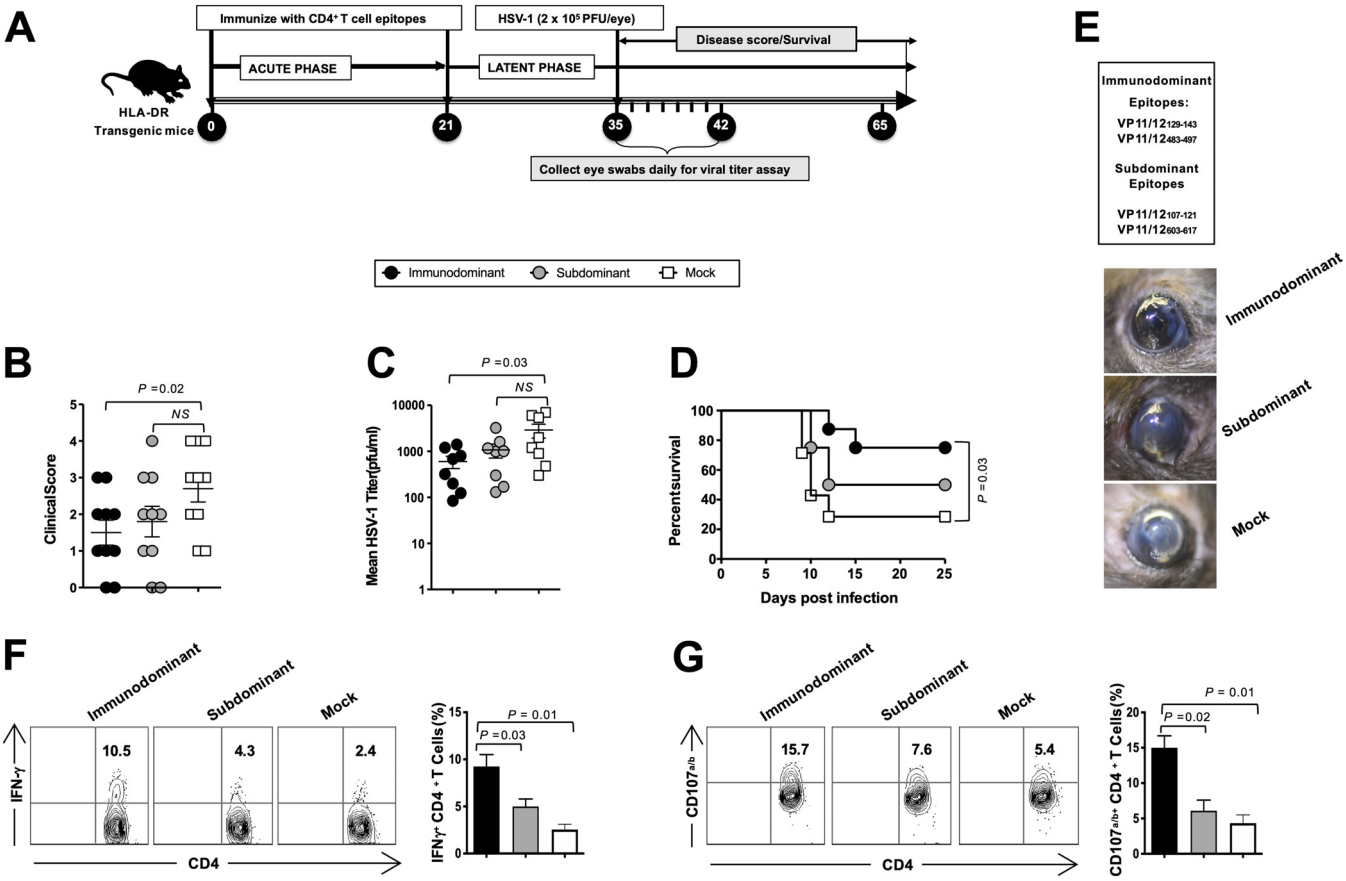

FIG 8 Protective immunity against ocular herpes infection and disease induced by immunodominant VP11/12 CD4$^+$ T epitopes in HLA-DR mice. (A) Timeline of immunization, HSV-1 infection, and immunological and virological analyses. Three groups of age-matched HLA-DR mice ($n = 10$ each) were immunized subcutaneously on days 0 and 21 with a mixture of two immunodominant human CD4$^+$ T cell peptides (VP11/12$_{129-143}$ and VP11/12$_{483-497}$) or with a mixture of two subdominant human CD4$^+$ T cell peptides (VP11/12$_{107-121}$ and VP11/12$_{603-617}$) emulsified in CpG$_{1826}$ adjuvant (100 μg of each peptide plus 2 μg of CpG$_{1826}$). The CpG$_{1826}$ adjuvant alone was used as control (mock vaccination). Two weeks after the final immunization, all animals were challenged ocularly with 2×10^5 PFU of HSV-1 (strain McKrae). (B) Shown is the average eye disease in peptide-immunized and mock-immunized mice 30 days postchallenge scored after the infection. (C) Virus titrations were determined from eye swabs on day 7 postinfection (the peak of viral replication). (D) Survival was determined in a window of 30 days postchallenge. (E) Representative images of ocular disease in HLA-DR mice immunized with the immunodominant and the subdominant peptide epitopes and in mock-immunized control mice. The functions of HSV-specific CD4$^+$ T cells were evaluated in the cornea from all three groups. (F) Representative FACS dot plots (left) and average (right) frequencies of IFN-γ^+CD4$^+$ T cells in the cornea of immunized and mock-immunized HLA-DR mice. (G) Representative FACS plots (left) and average (right) frequencies of CD107$^{a/b+}$ CD4$^+$ T cells in the cornea of immunized and mock-immunized HLA-DR mice. The *P* values (*, $P < 0.05$) indicate statistical significance between results for the mice immunized with immunodominant peptide epitopes and those of the mock control groups. The results are representative of two independent experiments.

(29–32). Mice with decreased CD4$^+$ T cell counts are prone to developing severe herpetic diseases (31). CD4$^+$ T helper cells play a major role in the development and maintenance of CD8$^+$ T cells and antibody (Ab)-mediated protective responses (33). CD4$^+$ T cells elicit various helper functions like priming and promotion of cytotoxic T lymphocytes and maintenance of effector memory CD8$^+$ T cells (34). Moreover, the CD4$^+$ T cells also help in the functioning and differentiation of B cells into plasmocytes that produce virus neutralizing antibodies (35, 36). However, in the past 2 decades, more attention has been given toward mapping and characterization of herpes CD8$^+$ T cell epitopes, with only a few studies focusing on mapping and characterization of herpes CD4$^+$ T cell epitopes. In the present study, we identified two previously unknown immunodominant VP11/12 CD4$^+$ T_{EM} cell epitopes, VP11/12$_{129-143}$ and VP11/12$_{483-497}$, using well-structured *in silico*, *in vitro*, and *in vivo* approaches. Remarkably, these effector VP11/12$_{129-143}$ and VP11/12$_{483-497}$ CD4$^+$ T cell epitopes were found to be less targeted by FOXP3$^+$ CD4$^+$ CD25$^+$ T_{reg} cells. Moreover, immunization of HLA-DR transgenic mice with a mixture of the two immunodominant human VP11/12 CD4$^+$ T_{EM} cell epitopes, but not with cryptic epitopes which are major targets

of T_{reg} cells, gave protection from ocular herpes infection and disease. To the best of our knowledge, this is the first report that demonstrates the extent of balance between the effector memory $CD4^+$ T cells and $FOXP3^+$ $CD4^+$ $CD25^+$ T_{reg} cells induced by a herpes vaccine, which determines protection from infection and disease.

Over the last 3 decades, clinical trials of herpes subunit vaccines have primarily focused on glycoproteins; results have been inconsistent, or the vaccines have failed to protect against herpes infection and disease (37). In addition to the 12 known herpes glycoproteins that are major targets of virus neutralizing antibodies, the tegument proteins appeared to be major targets of the HSV-specific $CD4^+$ and $CD8^+$ T cells. HSV tegument proteins are released into the cytoplasm during viral entry, making them one of the first viral proteins encountered by an infected cell and, therefore, an immediate target antigen (Ag) to induce host T cells. The HSV-1 virion protein 11/12 (VP11/12) is one of the most abundant tegument proteins and has emerged as an excellent antigen candidate for inducing protective immunity in animal models (38). In addition to their potential implication in a future herpes subunit immunotherapy and immunoprophylactic vaccine strategies, the VP11/12 $CD4^+$ T cell epitopes identified and characterized in the present study would also contribute to a better understanding of the correlates of human $CD4^+$ T cell responses with protection. Theoretically, numerous potential T cell epitopes could be generated from a protein antigen; however, in practice, T cells tend to focus upon just a few immunodominant regions. The VP11/12 $CD4^+$ T cell epitopes identified in this study are confined to three major immunodominant regions of the VP11/12 proteins, confirming our previous reports (39–49).

Eckles et al. have reported that the specificities of T cell responses to class II HLA molecules are heterogeneous, which may be influenced by different peptides occupying the HLA combining site and by the diversity of antigen-specific receptors of $CD4^+$ T cells recognizing the same HLA/peptide complex (50). Furthermore, a correlation between peptide binding to HLA-DR and $CD4^+$ T cell responses to the peptide epitopes in subjects of similar HLA-DR haplotypes has been established (51). Peptide-protein interactions play an essential role in T cell responses, T cell regulation, and signal transduction. It has been found that nearly 40% of the protein-protein interactions are mediated by short peptides; hence, determining the structure of protein-peptide complexes involved in these interactions would be crucial for understanding the molecular mechanism and subsequently modulating the protein-protein interactions for therapeutic purposes in herpes infection. In this context, we performed the protein-peptide docking experiment, which strengthens our data showing *in vitro* binding capacities of HSV-1 VP11/12-derived epitope peptides for soluble HLA-DR molecules. The highest protein-peptide binding interaction similarities were observed for the $VP11/12_{129-143}$ and $VP11/12_{483-497}$ epitopes, an *in silico* observation which we later confirmed functionally both *in vitro* and *in vivo*. Based on these *in silico* analyses, we screened 10 potential peptide epitopes with high predicted affinity to HLA-DRB1 molecules for *in vitro* studies. There exist numerous immunological assays, such as the ELISpot assay, IFN-γ intracellular assay, $CD107^{a/b}$ degranulation cytotoxic assay, and CFSE proliferation assay, which have been used to validate the functional significance of computationally predicted $CD4^+$ T cell epitopes (52–54). When used individually, each screen is not sufficient to conclusively identify functional $CD4^+$ T cell epitopes (52). However, combinations of multiple immunological screens provide strong evidence of functional $VP11/12_{129-143}$ and $VP11/12_{483-497}$ epitopes, as shown in other studies (54).

While the identification of epitopes is important for the development of prophylactic and therapeutic herpes subunit T cell-based vaccines, the existing approaches may overlook the effects of natural processing on epitope selection. Identification of immunodominant $CD4^+$ T cell epitopes using artificial peptides is challenging because they are often unable to recognize the native epitopes. This would be the result of multiple shortcomings, including the following: (i) the identified epitope may be cryptic; (ii) the artificial epitope is not processed or presented under natural conditions following HSV-1 infection of target cells; (iii) the T cell clone is inadvertently generated

against contaminants within the peptide preparation; and/or (iv) the T cell clone is in fact directed to cross-reactive epitopes between viruses within or outside the alpha herpes family, a phenomenon called heterologous immunity (55–57). Thus, identification of an epitope by sole means of *in vitro* binding to soluble HLA molecules and the *in vitro* T cell responses does not provide a firm indication as to whether or not the identified epitope will be naturally processed and presented to T cells by target cells following natural HSV-1 infection. In this study, we used a combination of multiple *in silico*, *in vitro*, and *in vivo* immunological screens to confirm that CD4$^+$ T cells specific to two identified epitopes, VP11/12$_{129-143}$ and VP11/12$_{483-497}$, specifically recognized native epitopes on HLA-DR-positive autologous dendritic cells when they were infected with HSV-1. We demonstrated *in vitro* binding capacities of VP11/12$_{129-143}$ and VP11/12$_{483-497}$ peptide epitopes to soluble HLA-DR molecules, a result that bolsters our *in silico* finding of epitope prediction and molecular docking that predicted the same epitopes as high-affinity binders to most common HLA-DRB1 molecules.

In the present study, the immunodominant VP11/12$_{129-143}$ and VP11/12$_{483-497}$ CD4$^+$ T cell epitopes identified using the TEPITOPE strategy were confirmed using the PepScan library mapping strategy. Thus, using the traditional yet robust overlapping peptide screening approach to identify any missing epitopes from the entire sequence of a VP11/12 protein antigen, which was otherwise not predicted using computational tools, confirmed the same epitopes. Moreover, we generated CD4$^+$ T cell lines specific to VP11/12$_{129-143}$ and VP11/12$_{483-497}$ epitopes and demonstrated that they undergo significant CD107$^{a/b}$ degranulation and produced higher levels of IFN-γ when incubated with HLA-DR-positive autologous target DC infected with HSV-1. Finally, we confirmed these *in silico* and *in vitro* results by demonstrating that immunization of HLA-DR transgenic mice with a mixture of the two immunodominant VP11/12$_{129-143}$ and VP11/12$_{483-497}$ CD4$^+$ T cell epitopes induced protective multifunctional CD4$^+$ T cells, associated with a decrease in ocular herpes infection and disease.

Over the last 25 years, several types of herpes vaccines have been attempted, eliciting mostly strong systemic antibody responses. However, in clinical trials, they failed to protect therapeutically or prophylactically. The TG and ocular epithelial tissues are the most obvious battlefield sites for the host's B and T cells to control recurrent HSV-1. In addition to neutralizing antibodies and antiviral effector CD8$^+$ T cells, CD4$^+$ T cells appear to be critical in preventing or aborting virus reactivations from latently infected neurons of TG (designated central neuronal immunity) (49). Studies in the HSV-infected animal model and observations in HSV-1-infected asymptomatic individuals without recurrent herpetic diseases point to the presence of both CD4$^+$ and CD8$^+$ T cells at the healed sites of the epithelia. Antiviral effector CD4$^+$ T cells play a direct role in preventing virus replication either through production of IFN-γ or through cytotoxic activity. Activated CD4$^+$ T cells are also retained in the latently infected TG of mice and humans (49). Effector CD4$^+$ T cells may also limit virus replication in the corneal epithelium (designated peripheral epithelial immunity). CD4$^+$ T helper cells are a source of large amounts of cytokines that promote generation and maintenance of antiviral memory CD8$^+$ T cells, thus indirectly contributing to protection (13).

The mechanisms by which HSV-specific CD4$^+$ T cells gave protection from ocular herpes infection and disease remain to be fully determined. We demonstrated that induction of VP11/12$_{129-143}$ and VP11/12$_{483-497}$ epitope-specific CD4$^+$ T cells in the cornea correlated with protection. Carbone's group has demonstrated that, following skin infection, memory CD4$^+$ T cells migrate between the blood and infected skin, while CD8$^+$ memory cells remain localized in infected tissue (58–60). Therefore, increasing the number of circulating HSV-specific CD4$^+$ T cells in the cornea and even in the TG, where they may contribute to preventing virus reactivation during latency, would be a prerequisite for an effective epitope-based herpes vaccine. We are currently investigating reopening the cornea (peripheral corneal immunity) and latently infected TG (central neuronal immunity) to infiltration by antiviral CD4$^+$ and CD8$^+$ T cells by increasing levels of T cell-attracting CXCL9, CXCL10, or CXCL11. We will accomplish this

by inducing expression of these T cell-attracting chemokines locally, either in cornea or in TG, under tissue-specific epithelial and neurotropic promoters. Results from this approach, which we designate peripheral epithelial immunity and central neuronal immunity, respectively, will be the subject of future reports.

Safety concerns, such as autoimmunity, have been associated with systemic injections of monoclonal antibodies (MAbs) to block immune checkpoints. Thus, in addition to systemic injection of blockade MAbs, a direct delivery of single-chain variable-fragment Fc (scFv-Fc) Abs using engendered adeno-associated virus (AAV) vectors may avoid unwanted systemic immune-related adverse events (IRAE) associated with the use of systemically delivered checkpoint inhibitors (61). If local delivery of LAG-3 and PD-1 checkpoint inhibitors directly into cornea and TG causes uncontrolled local inflammation, we are currently considering using an inducible tissue-specific promoter that will be turned on/off (62) or selectively stimulated by reactivated HSV-1 locally within TG (63). Moreover, the timing of delivery and dosage of blockade MAbs that would result in clinical efficacy with little to no side effects are being considered, and the results will be the subject of future reports.

In conclusion, our findings report two, previously unknown epitopes derived from the HSV-1 VP11/12 protein that tend to recall polyfunctional effector memory $CD4^+$ T_{EM} cell responses in HSV-seropositive asymptomatic individuals. The results show quantitative and qualitative features of an effective HSV-specific $CD4^+$ T cell response that should be considered in the next generation of herpes vaccine studies.

MATERIALS AND METHODS

Human study population. All clinical investigations in this study were conducted according to the Declaration of Helsinki. All subjects were enrolled at the University of California, Irvine, under an approved Institutional Review Board protocol (IRB 2009-6963). Written informed consent was received from all participants prior to inclusion in the study. During the last 15 years (i.e., January 2003 to September 2019), we screened 925 asymptomatic individuals for HSV-1 and HSV-2 seropositivity. A total of 587 were White, 338 were non-White (African, Asian, Hispanic, and other), 458 were female, and 467 were male. Among these participants, a cohort of 726 immuno-competent asymptomatic individuals, ranging from 21 to 67 years old (median age, 39 years), were seropositive for HSV-1 and seronegative for HSV-2. All patients were negative for HIV and hepatitis B virus (HBV), with no history of immunodeficiency. A total of 792 patients were HSV-1, HSV-2, or HSV-1/HSV-2 seropositive, among which 698 patients were healthy and defined as asymptomatic. Based on self-reporting and clinical examination, these patients never had any herpes disease (ocular, genital, or dermal). Even a single episode of any herpetic disease excluded the individual from this group. No attempt was made to assign specific T cell epitopes to the severity of recurrent lesions. Patients were also excluded if they (i) had an active ocular (or elsewhere) herpetic lesion or had had one within the past 30 days, (ii) were seropositive for HSV-2, (3) were pregnant or breastfeeding, or (4) were on acyclovir and other related antiviral drugs or any other immunosuppressive drugs at the time of blood draw. Among this large cohort of healthy seropositive asymptomatic individuals, 50 patients were enrolled in the current study (Table 3).

HSV-specific serotyping. The serum samples collected from random donors were tested for anti-HSV antibodies. An enzyme-linked immunosorbent assay (ELISA) was performed on sterile 96-well flat-bottom microplates coated with the HSV-1 antigen in coating buffer overnight at 4°C. The next day, plates were washed with phosphate-buffered saline (PBS)–1% Tween 20 (PBST) five times, and nonspecific binding was blocked by incubation with a 5% solution of skimmed milk in PBS (200 μl/well) at 4°C for 1 h at room temperature (RT). The microplates were washed three times with PBS-Tween and incubated with various sera at 37°C for 2 h. Following five washes, biotinylated rabbit anti-human IgG, diluted 1:20,000 with PBST, was incubated at 37°C for 2 h. After five washes, streptavidin was added at a 1:5,000 dilution and incubated for 30 min at RT. After five additional washes, the color was developed by adding 100 μl of 3,3′,5,5′-tetramethylbenzidine (TMB) substrate. The mixture was incubated for 5 to 15 min at RT in the absence of light. The reaction was terminated by adding 1 M H_2SO_4. Absorbance was measured at 450 nm.

Bioinformatics analyses. HSV-1 VP11/12 open reading frames used in this study were from strain 17 (NCBI accession no. P10230). The 718-aa sequence (Fig. 1) of the VP11/12 protein was screened for (HLA)-DR-restricted epitopes using different computational algorithms, as previously described (26, 27).

TEPITOPE algorithm. The VP11/12 sequence (HSV-1 strain 17) was loaded into the new prediction software (TEPITOPE) to predict $CD4^+$ epitopes (2). The TEPITOPE algorithm is a Windows application that is based on 25 quantitative matrix-based motifs that cover a significant part of human HLA class II peptide binding specificity (2). The algorithm permits the prediction and parallel display of ligands for each of the 25 HLA-DR alleles. The TEPITOPE prediction threshold was set at 5%, and 10 regions, predicted to bind at least 50% of the major histocompatibility complex (MHC) class II molecules, were picked.

PepScan peptide library screening and synthesis. VP11/12 (strain 17; NCBI accession no. P10230) was used in this study. Eighty-nine synthetic peptides encompassing the entire sequence of HSV-1

TABLE 3 Cohorts of HLA-DR-positive, HSV-seropositive asymptomatic individuals enrolled in this study

Subject-level parameter	Value for the parameter ($n = 50$)
Gender (no. [%])	
Female	32 (64)
Male	18 (36)
Race (no. [%])	
Caucasian	28 (56)
Non-Caucasian	22 (44)
Median age (yr [range])	39 (21–67)
HSV status (no. [%])	
HSV-2 seropositive	0 (0)
HSV-1 seropositive	50 (100)
HLA status (no. [%])	
HLA-DR positive	50 (100)
HLA-DR negative	0 (0)
Herpes disease status (no. [%])	
Asymptomatic	50 (100)

VP11/12 (718 aa) were produced by using the Multipin DKP system (Mimotopes, San Diego, CA). Figure 4 show examples of the 10 overlapping peptides forming pool 1 to pool 9. Peptides were synthesized as 18- to 22-mers, overlapping by 10 amino acids with adjacent peptides. This synthesis was performed using classical Fmoc/tBu [(9-fluorenylmethoxy carbonyl)/*tert*-butyl] chemistry. After side-chain deprotection with a mixture of trifluoroacetic acid, ethanedithiol, and anisole (38:1:1), the peptides were cleaved in an ammonium bicarbonate buffer (0.1 M, pH 8.4) with 40% (vol/vol) acetonitrile via a cyclization mechanism, leaving a cyclo(lysylpropyl) moiety at the C terminus. Lastly, the peptides were freeze-dried and stored as a dry powder at −80°C. Working stock solutions of the peptides were made at 1 mg/ml in PBS–10% dimethyl sulfoxide (DMSO) and were stored at −20°C.

HLA-DR typing. The HLA-DR status was confirmed by staining PBMCs with 2 ml of anti-HLA-DR MAb (clone BB7.2; BD Pharmingen) at 4°C for 30 min. The cells were then washed and analyzed by flow cytometry using an LSRII instrument (Becton, Dickinson). The acquired data were analyzed with FlowJo software (BD Biosciences, San Jose, CA).

Molecular peptide docking. Computational peptide docking of CD4 peptides (VP11/12$_{107–121}$, VP11/12$_{129–143}$, VP11/12$_{138–152}$, VP11/12$_{144–158}$, VP11/12$_{264–278}$, VP11/12$_{465–479}$, VP11/12$_{483–497}$, VP11/12$_{493–507}$, VP11/12$_{519–533}$, and VP11/12$_{603–617}$) into the HLA-DRB1 complex (binding protein) was performed using GalaxyPepDock under GalaxyWEB (64). To retrieve the HLA-DR1 structure, we used the X-ray crystallographic structure of the HLA-DM-HLA-DR1 complex (PDB accession number 4GBX) (65). The 4GBX protein with a structural weight of 92,814.37 Da, possesses five unique protein chains, 811 residues, and 6,130 atoms. In this study, flexible target docking based on an energy optimization algorithm was carried out on the ligand-binding domain containing HLA-DRB1 within the 4GBX structure. Similarly, scores were calculated for protein-peptide interaction pairs for each residue. Subsequently, molecular docking models were built based on distance restraints for protein-peptide pairs using GalaxyPepDock (64). Docking models were ranked based on optimized energy scores.

Peptide binding assays specific for HLA-DR molecules. HLA-DR molecules were immunopurified from homologous Epstein-Barr virus (EBV) cell lines by affinity chromatography using the monomorphic MAbs L243 and B7/21, as previously reported (66–69). The binding to HLA-DR molecules was assessed by competitive ELISA using biotinylated VP11/12 peptides as previously reported (70). Unlabeled forms of nonherpes peptides were used as a reference to assess the validity of each experiment. The sequences of these reference peptides and IC_{50} values are as follows: hemagglutinin (HA) residues 306 to 318 (PKYVKQNTLKLAT), IC_{50}s of 1 nM for DRB1*0101, 5 nM for DRB1*0401, and 11 nM for DRB1*1101; YKL (AAYAAAKAAALAA), IC_{50} of 10 nM for DRB1*0701; A3 residues 152 to 166 (EAEQLRAYLDGTGVE), IC_{50} of 35 nM for DRB1*1501; MT residues 2 to 16 (AKTIAYDEEARRGLE), IC_{50} of 129 nM for DRB1*0301; B1 residues 21 to 36 (TERVRLVTRHIYNREE), IC_{50} of 52 nM for DRB1*1301.

PBMCs: preparation and ELISpot assay. Peripheral blood mononuclear cells (PBMCs) were isolated, as we have previously described (25). Approximately 100 ml of the donor's blood was drawn into yellow-top Vacutainer tubes (Becton, Dickinson, Franklin Lakes, NJ). The serum was isolated and centrifuged for 10 min at 800 × *g*. The PBMCs were isolated by gradient centrifugation using leukocyte separation medium (Corning, Tewksbury, MA). The cells were then washed in PBS and resuspended in complete culture medium. Aliquots of freshly isolated PBMCs were also cryopreserved in liquid nitrogen for future testing.

T cell stimulation was measured by IFN-γ production in peptide-stimulated PBMCs using a BD ELISpot IFN-γ kit (BD-Pharmingen, San Diego, CA), as we have previously described (25). Briefly, 3×10^5 PBMCs were stimulated for 2 days with 10 μg/ml of pooled peptides (10 peptides per pool), with 10 μg/ml of an

individual VP11/12 peptide, with heat-inactivated HSV-1 (strain McKrae) (multiplicity of infection [MOI] of 5), or with 1 μg/ml PHA as a positive control, in ELISpot plates (Merck Millipore, Billerica, MA). These plates were precoated with anti-human IFN-γ capture Ab in a humidified incubator at 37°C with 5% CO_2. The spot-forming cells were developed as described by the manufacturer (ELISpot IFN-γ kit; BD-Pharmingen) and counted using an automated ELISpot reader (ImmunoSpot).

T cell activation and proliferation. PBMCs were stained with CFSE (2 mM) and then incubated with individual VP11/12 peptides (10 μg/ml) for 5 days. The cells were then washed and stained for CD4 molecule expression. Cycling cells were then analyzed by flow cytometry, and their absolute numbers were calculated using the following formula: (number of events in double-positive cells) $\times$ (number of events in gated lymphocytes)/(number of total events acquired).

Generation of VP11/12 peptide-specific CD4$^+$ T cell lines. PBMC-derived DCs were generated using the cytokines interleukin-4 (IL-4) and granulocyte-macrophage colony-stimulating factor (GM-CSF) and pulsed with different HSV-1 VP11/12 peptides (10 μg/ml). DC were then stimulated with autologous CD4$^+$ T cells and irradiated autologous feeder cells. Recombinant human IL-2 (100 IU/ml; Peprotech) was added to the culture every fifth day starting on day 5. Fourteen days after initial contact, cells were restimulated using autologous immature DC (imDC) (1:20, DC/CD4$^+$ T cell ratio) pulsed again with the same HSV-1 VP11/12 peptides and irradiated autologous feeder cells (5:1, feeder/CD4$^+$ T cell ratio). Peptide specificities of the CD4$^+$ T cell lines were tested 10 days later, and T cells were first put in coculture with autologous DC and pulsed with the two different HSV-1 peptides (VP11/12$_{129-143}$ and (VP11/12$_{483-497}$) or one control peptide (VP11/12$_{107-121}$) under three separate conditions; the T-cell response was measured by IFN-γ ELISpot assay and intracellular FACS staining.

Generation of autologous target cells. To obtain autologous DC, mononuclear cells isolated from human blood samples were initially plated in serum-free medium (Life Technologies) for 2 h in a six-well plate at an initial density of 1×10^6 cells/ml in a final volume of 3 ml per well. Nonadherent cells were subsequently removed by three successive washes with 1$\times$ cold PBS, and the adherent monocytes were then cultured in RPMI 1640 medium with 10% fetal bovine serum (FBS) supplemented with human GM-CSF (50 ng/ml) and IL-4 (5 ng/ml) (PeproTech Inc., Rocky Hill, NJ). After 5 to 6 days, over 90% of the nonadherent cells had acquired typical dendritic morphology. PBMC-derived autologous DC were then infected overnight with HSV-1, each at a multiplicity (MOI) of infection of 0.1 and 1. The next day, infected DC were washed three times and incubated with effector CD4$^+$ T cell lines at an effector/target (E/T) ratio of 1:5 for 4 h. The cytotoxic activity was detected by a CD107$^{a/b}$ degranulation assay, and the T cell response was measured by IFN-γ ELISpot assay and intracellular FACS staining.

T cell assay. To detect cytolytic CD4$^+$ T cells recognizing VP11/12 peptides in freshly isolated human PBMCs and mouse corneal cells, we used a CD107$^{a/b}$ cytotoxicity assay, as we have recently described (25). On the day of the assay, nonstimulated or VP11/12 peptide-stimulated PBMCs were incubated at 37°C for 5 to 6 h with BD GolgiStop, costimulatory Abs anti-CD28 and anti-CD49d (1 μg/ml), and 10 μl of CD107a-fluorescein isothiocyanate (FITC) and CD107b-FITC (clone LAMP; BioLegend, San Diego, CA). At the end of the incubation period, cells were harvested into separate tubes and washed once with FACS buffer and then stained with allophycocyanin (APC)-conjugated anti-human CD4 (clone OKT4) for 30 min. The cells were then rewashed and analyzed using an LSRII instrument (Becton, Dickinson, San Diego, CA). Cells from mouse cornea were also analyzed by flow cytometry after staining with phycoerythrin (PE)-Cy7 fluorochrome-conjugated mouse-specific CD4 MAb (clone GK1.5).

HLA-DR transgenic mice. All animal studies were conducted in facilities approved by the Association for Assessment and Accreditation of Laboratory Animal Care and according to an Institutional Animal Care and Use Committee-approved animal protocol (IACUC approval AUP19-111). HLA-DR transgenic mice, previously described (8, 71), were kindly provided by Francois Lemonier (Pasteur Institute, Paris, France) and were bred at the University of California, Irvine.

Virus production. HSV-1 (lab strain McKrae) was grown and titrated on rabbit skin (RS) cells. UV-inactivated HSV-1 was generated, and HSV inactivation was confirmed by the inability to produce plaques when virus was tested on RS cells.

Immunization of HLA-DR mice with VP11/12 peptide epitopes. Three groups of age-matched female HLA-DR mice ($n = 10$ each) were immunized subcutaneously with the immunodominant CD4$^+$ T cell human epitopes (VP11/12$_{129-143}$ and VP11/12$_{483-497}$) emulsified in CpG$_{1826}$ adjuvant, with the subdominant CD4$^+$ T cell human epitopes (VP11/12$_{107-121}$ and VP11/12$_{603-617}$) emulsified in CpG$_{1826}$ adjuvant or with the CpG$_{1826}$ adjuvant alone (mock) on days 0 and 21. All immunizations were carried out with 100 μM each peptide. Two weeks after the second and final immunizations, animals from all groups received an ocular HSV-1 challenge (2×10^5 PFU, McKrae strain) without scarification. The mice were then assessed for up to 30 days postchallenge for ocular herpes pathology, ocular viral titers, and survival.

Monitoring of ocular herpes virus infection and disease. Animals were examined for signs of ocular disease by slit lamp. Clinical assessments were made immediately postinoculation and on days 1, 3, 5, 7, 10, 14, and 21 thereafter. The examination was performed by investigators blinded to the treatment regimen of the mice and scored according to a standard scale of 0 to 4: 0, no disease; 1, 25%; 2, 50%; 3, 75%; and 4, 100% staining. To quantify replication and clearance of HSV-1 from the eyes, mice were swabbed daily with moist, type 1 calcium alginate swabs. Swabs were placed in 1.0 ml of titration medium (Dulbecco's modified Eagle medium [DMEM], 2% penicillin-streptomycin, 5% fetal bovine serum) and frozen at -80°C until titrated on RS cell monolayers. Mice were also examined for survival in a window of 30 days after the challenge.

Statistical analyses. Data for each assay were compared by analysis of variance (ANOVA) and Student's *t* test using GraphPad Prism, version 5 (La Jolla, CA). Differences between the groups were

identified by ANOVA and multiple-comparison procedures, as we previously described (72). Data are expressed as the means ± standard deviations (SD). Results were considered statistically significant at a *P* value of <0.05.

ACKNOWLEDGMENTS

This work is supported by Public Health Service Research grants EY026103, EY019896, and EY024618 from the National Eye Institute, by grants AI143348, AI147499, AI143326, AI138764, AI124911, and AI110902 from the National Institutes of Allergy and Infectious Diseases (NIAID), and in part by a Discovery Center for Eye Research and Research to Prevent Blindness grant.

This work is dedicated to the memory of the late Steven L. Wechsler (1948–2016), whose numerous pioneering works on herpesvirus infection and immunity laid the foundation for this line of research.

We thank the NIH Tetramer Facility (Emory University, Atlanta, GA) for providing the tetramers used in this study and Angele Nalbandian (Gavin Herbert Eye Institute, University of California Irvine, Irvine, CA) for help editing the manuscript.

We declare that no conflict of interest exists.

REFERENCES

1. Looker KJ, Magaret AS, May MT, Turner KME, Vickerman P, Gottlieb SL, Newman LM. 2015. Global and regional estimates of prevalent and incident herpes simplex virus type 1 infections in 2012. PLoS One 10:e0140765. https://doi.org/10.1371/journal.pone.0140765.
2. BenMohamed L, Bertrand G, McNamara CD, Gras-Masse H, Hammer J, Wechsler SL, Nesburn AB. 2003. Identification of novel immunodominant CD4$^+$ Th1-type T-cell peptide epitopes from herpes simplex virus glycoprotein D that confer protective immunity. J Virol 77:9463–9473. https://doi.org/10.1128/jvi.77.17.9463-9473.2003.
3. Zhang X, Issagholian A, Berg EA, Fishman JB, Nesburn AB, BenMohamed L. 2005. Th-cytotoxic T-lymphocyte chimeric epitopes extended by N^{ε}-palmitoyl lysines induce herpes simplex virus type 1-specific effector CD8$^+$ Tc1 responses and protect against ocular infection. J Virol 79:15289–15301. https://doi.org/10.1128/JVI.79.24.15289-15301.2005.
4. Nesburn AB, Bettahi I, Zhang X, Zhu X, Chamberlain W, Afifi RE, Wechsler SL, BenMohamed L. 2006. Topical/mucosal delivery of sub-unit vaccines that stimulate the ocular mucosal immune system. Ocul Surf 4:178–187. https://doi.org/10.1016/s1542-0124(12)70164-7.
5. Harrison KS, Zhu L, Thunuguntla P, Jones C, Harrison KS, Zhu L, Thunuguntla P, Jones C. 2019. Antagonizing the glucocorticoid receptor impairs explant-induced reactivation in mice latently infected with herpes simplex virus 1. J Virol 93:e00418-19. https://doi.org/10.1128/JVI.00418-19.
6. Wilhelmus KR, Beck RW, Moke PS, Dawson CR, Barron BA, Jones DB, Kaufman HE, Kurinij N, Stulting D, Sugar J, Cohen EJ, Hyndiuk RA, Asbell PA, Herpetic Eye Disease Study Group. 1998. Acyclovir for the prevention of recurrent herpes simplex virus eye disease. N Engl J Med 339:300–306. https://doi.org/10.1056/NEJM199807303390503.
7. Rao P, Suvas S. 2019. Development of inflammatory hypoxia and prevalence of glycolytic metabolism in progressing herpes stromal keratitis lesions. J Immunol 202:514–526. https://doi.org/10.4049/jimmunol.1800422.
8. Kuo T, Wang C, Badakhshan T, Chilukuri S, BenMohamed L. 2014. The challenges and opportunities for the development of a T-cell epitope-based herpes simplex vaccine. Vaccine 32:6733–6745. https://doi.org/10.1016/j.vaccine.2014.10.002.
9. Dix RD. 1987. Prospects for a vaccine against herpes simplex virus types 1 and 2. Prog Med Virol 34:89–128.
10. St Leger AJ, Jeon S, Hendricks RL. 2013. Broadening the repertoire of functional herpes simplex virus type 1-specific CD8$^+$ T cells reduces viral reactivation from latency in sensory ganglia. J Immunol 191:2258–2265. https://doi.org/10.4049/jimmunol.1300585.
11. St Leger AJ, Peters B, Sidney J, Sette A, Hendricks RL. 2011. Defining the herpes simplex virus-specific CD8$^+$ T cell repertoire in C57BL/6 mice. J Immunol 186:3927–3933. https://doi.org/10.4049/jimmunol.1003735.
12. Vahed H, Agrawal A, Srivastava R, Prakash S, Coulon PA, Roy S, BenMohamed L. 2019. Unique type I interferon, expansion/survival cytokines, and JAK/stat gene signatures of multifunctional herpes simplex virus-specific effector memory CD8$^+$ TEM cells are associated with asymptomatic herpes in humans. J Virol 93:e01882-18. https://doi.org/10.1128/JVI.01882-18.
13. Srivastava R, Roy S, Coulon PA, Vahed H, Prakash S, Dhanushkodi N, Kim GJ, Fouladi MA, Campo J, Teng AA, Liang X, Schaefer H, BenMohamed L. 2019. Therapeutic mucosal vaccination of HSV-2 infected guinea pigs with the ribonucleotide reductase 2 (RR2) protein boosts antiviral neutralizing antibodies and tissue-resident CD4$^+$ and CD8$^+$ TRM cells associated with protection against recurrent genital herpes. J Virol 93:e02390-18. https://doi.org/10.1128/JVI.02309-18.
14. Roy S, Coulon PG, Prakash S, Srivastava R, Geertsema R, Dhanushkodi N, Lam C, Nguyen V, Gorospe E, Nguyen AM, Salazar S, Alomari NI, Warsi WR, BenMohamed L. 2019. Blockade of PD-1 and LAG-3 immune checkpoints combined with vaccination restore the function of anti-viral tissue-resident CD8$^+$ TRM cells and reduce ocular herpes simplex infection and disease in HLA Transgenic rabbits. J Virol 93:e00827-19. https://doi.org/10.1128/JVI.00827-19.
15. Rajasagi NK, Kassim SH, Kollias CM, Zhao X, Chervenak R, Jennings SR. 2009. CD4$^+$ T cells are required for the priming of CD8$^+$ T cells following infection with herpes simplex virus type 1. J Virol 83:5256–5268. https://doi.org/10.1128/JVI.01997-08.
16. Johnson AJ, Chu CF, Milligan GN. 2008. Effector CD4$^+$ T cell involvement in clearance of infectious herpes simplex virus type 1 from sensory ganglia and spinal cords. J Virol 82:9678–9688. https://doi.org/10.1128/JVI.01159-08.
17. Belshe RB, Leone PA, Bernstein DI, Wald A, Levin MJ, Stapleton JT, Gorfinkel I, Morrow RL, Ewell MG, Stokes-Riner A, Dubin G, Heineman TC, Schulte JM, Deal CD, Herpevac Trial for Women. 2012. Efficacy results of a trial of a herpes simplex vaccine. N Engl J Med 366:34–43. https://doi.org/10.1056/NEJMoa1103151.
18. Stanberry LR. 2004. Clinical trials of prophylactic and therapeutic herpes simplex virus vaccines. Herpes 11(Suppl 3):161A–169A.
19. Van Wagoner N, Fife K, Leone PA, Bernstein DI, Warren T, Panther L, Novak RM, Beigi R, Kriesel J, Tyring S, Koltun W, Lucksinger G, Morris A, Zhang B, McNeil LK, Tasker S, Hetherington S, Wald A. 2018. Effects of different doses of GEN-003, a therapeutic vaccine for genital herpes simplex virus-2, on viral shedding and lesions: results of a randomized placebo-controlled trial. J Infect Dis 218:1890–1899. https://doi.org/10.1093/infdis/jiy415.
20. Bernstein DI, Wald A, Warren T, Fife K, Tyring S, Lee P, Van Wagoner N, Magaret A, Flechtner JB, Tasker S, Chan J, Morris A, Hetherington S. 2017. Therapeutic vaccine for genital herpes simplex virus-2 infection: findings from a randomized trial. J Infect Dis 215:856–864. https://doi.org/10.1093/infdis/jix004.
21. Stanberry LR, GlaxoSmithKline Herpes Vaccine Efficacy Study Group, Spruance SL, Cunningham AL, Bernstein DI, Mindel A, Sacks S, Tyring S, Aoki FY, Slaoui M, Denis M, Vandepapeliere P, Dubin G, GlaxoSmithKline Herpes Vaccine Efficacy Study G. 2002. Glycoprotein-D-adjuvant vaccine

to prevent genital herpes. N Engl J Med 347:1652–1661. https://doi.org/10.1056/NEJMoa011915.
22. Hosken N, McGowan P, Meier A, Koelle DM, Sleath P, Wagener F, Elliott M, Grabstein K, Posavad C, Corey L. 2006. Diversity of the CD8+ T-cell response to herpes simplex virus type 2 proteins among persons with genital herpes. J Virol 80:5509–5515. https://doi.org/10.1128/JVI.02659-05.
23. Long D, Skoberne M, Gierahn TM, Larson S, Price JA, Clemens V, Baccari AE, Cohane KP, Garvie D, Siber GR, Flechtner JB. 2014. Identification of novel virus-specific antigens by CD4+ and CD8+ T cells from asymptomatic HSV-2 seropositive and seronegative donors. Virology 464–465:296–311. https://doi.org/10.1016/j.virol.2014.07.018.
24. Dasgupta G, Chentoufi AA, Kalantari M, Falatoonzadeh P, Chun S, Lim CH, Felgner PL, Davies DH, BenMohamed L. 2012. Immunodominant "asymptomatic" herpes simplex virus 1 and 2 protein antigens identified by probing whole-ORFome microarrays with serum antibodies from seropositive asymptomatic versus symptomatic individuals. J Virol 86:4358–4369. https://doi.org/10.1128/JVI.07107-11.
25. Kalantari-Dehaghi M, Chun S, Chentoufi AA, Pablo J, Liang L, Dasgupta G, Molina DM, Jasinskas A, Nakajima-Sasaki R, Felgner J, Hermanson G, BenMohamed L, Felgner PL, Davies DH. 2012. Discovery of potential diagnostic and vaccine antigens in herpes simplex virus 1 and 2 by proteome-wide antibody profiling. J Virol 86:4328–4339. https://doi.org/10.1128/JVI.05194-11.
26. Posavad CM, Wald A, Hosken N, Huang ML, Koelle DM, Ashley RL, Corey L. 2003. T cell immunity to herpes simplex viruses in seronegative subjects: silent infection or acquired immunity? J Immunol 170:4380–4388. https://doi.org/10.4049/jimmunol.170.8.4380.
27. Verjans GM, Dings ME, McLauchlan J, van Der Kooi A, Hoogerhout P, Brugghe HF, Timmermans HA, Baarsma GS, Osterhaus AD. 2000. Intraocular T cells of patients with herpes simplex virus (HSV)-induced acute retinal necrosis recognize HSV tegument proteins VP11/12 and VP13/14. J Infect Dis 182:923–927. https://doi.org/10.1086/315759.
28. Verjans GM, Remeijer L, Mooy CM, Osterhaus AD. 2000. Herpes simplex virus-specific T cells infiltrate the cornea of patients with herpetic stromal keratitis: no evidence for autoreactive T cells. Invest Ophthalmol Vis Sci 41:2607–2612.
29. Gangappa S, Deshpande SP, Rouse BT. 1999. Bystander activation of CD4+ T cells can represent an exclusive means of immunopathology in a virus infection. Eur J Immunol 29:3674–3682. https://doi.org/10.1002/(SICI)1521-4141(199911)29:11<3674::AID-IMMU3674>3.0.CO;2-7.
30. Kwok WW, Gebe JA, Liu A, Agar S, Ptacek N, Hammer J, Koelle DM, Nepom GT. 2001. Rapid epitope identification from complex class-II-restricted T-cell antigens. Trends Immunol 22:583–588. https://doi.org/10.1016/s1471-4906(01)02038-5.
31. Manickan E, Rouse BT. 1995. Roles of different T-cell subsets in control of herpes simplex virus infection determined by using T-cell-deficient mouse-models. J Virol 69:8178–8179. https://doi.org/10.1128/JVI.69.12.8178-8179.1995.
32. Mikloska Z, Cunningham AL. 1998. Herpes simplex virus type 1 glycoproteins gB, gC and gD are major targets for CD4 T-lymphocyte cytotoxicity in HLA-DR expressing human epidermal keratinocytes. J Gen Virol 79:353–361. https://doi.org/10.1099/0022-1317-79-2-353.
33. Delvig AA, Robinson JH. 2001. CD4 T-cell epitope mapping. Methods Mol Med 66:349–360. https://doi.org/10.1385/1-59259-148-5:349.
34. BenMohamed L, Krishnan R, Longmate J, Auge C, Low L, Primus J, Diamond DJ. 2000. Induction of CTL response by a minimal epitope vaccine in HLA A*0201/DR1 transgenic mice: dependence on HLA class II restricted T(H) response. Hum Immunol 61:764–779. https://doi.org/10.1016/s0198-8859(00)00139-7.
35. Hook LM, Awasthi S, Dubin J, Flechtner J, Long D, Friedman HM. 2019. A trivalent gC2/gD2/gE2 vaccine for herpes simplex virus generates antibody responses that block immune evasion domains on gC2 better than natural infection. Vaccine 37:664–669. https://doi.org/10.1016/j.vaccine.2018.11.076.
36. Bernstein DI, Pullum DA, Cardin RD, Bravo FJ, Dixon DA, Kousoulas KG. 2019. The HSV-1 live attenuated VC2 vaccine provides protection against HSV-2 genital infection in the guinea pig model of genital herpes. Vaccine 37:61–68. https://doi.org/10.1016/j.vaccine.2018.11.042.
37. Chentoufi AA, Kritzer E, Yu DM, Nesburn AB, BenMohamed L. 2012. Towards a rational design of an asymptomatic clinical herpes vaccine: the old, the new, and the unknown. Clin Dev Immunol 2012:187585. https://doi.org/10.1155/2012/187585.
38. Murphy MA, Bucks MA, O'Regan KJ, Courtney RJ. 2008. The HSV-1 tegument protein pUL46 associates with cellular membranes and viral capsids. Virology 376:279–289. https://doi.org/10.1016/j.virol.2008.03.018.
39. Chentoufi AA, Zhang X, Lamberth K, Dasgupta G, Bettahi I, Nguyen A, Wu M, Zhu X, Mohebbi A, Buus S, Wechsler SL, Nesburn AB, BenMohamed L. 2008. HLA-A*0201-restricted CD8+ cytotoxic T lymphocyte epitopes identified from herpes simplex virus glycoprotein D. J Immunol 180:426–437. https://doi.org/10.4049/jimmunol.180.1.426.
40. Bettahi I, Dasgupta G, Renaudet O, Chentoufi AA, Zhang X, Carpenter D, Yoon S, Dumy P, BenMohamed L. 2009. Antitumor activity of a self-adjuvanting glyco-lipopeptide vaccine bearing B cell, CD4+ and CD8+ T cell epitopes. Cancer Immunol Immunother 58:187–200. https://doi.org/10.1007/s00262-008-0537-y.
41. Chentoufi AA, Dervillez X, Rubbo PA, Kuo T, Zhang X, Nagot N, Tuaillon E, Van De Perre P, Nesburn AB, BenMohamed L. 2012. Current trends in negative immuno-synergy between two sexually transmitted infectious viruses: HIV-1 and HSV-1/2. Curr Trends Immunol 13:51–68.
42. Dervillez X, Qureshi H, Chentoufi AA, Khan AA, Kritzer E, Yu DC, Diaz OR, Gottimukkala C, Kalantari M, Villacres MC, Scarfone VM, McKinney DM, Sidney J, Sette A, Nesburn AB, Wechsler SL, BenMohamed L. 2013. Asymptomatic HLA-A*02:01-restricted epitopes from herpes simplex virus glycoprotein B preferentially recall polyfunctional CD8+ T cells from seropositive asymptomatic individuals and protect HLA transgenic mice against ocular herpes. J Immunol 191:5124–5138. https://doi.org/10.4049/jimmunol.1301415.
43. Srivastava R, Dervillez X, Khan AA, Chentoufi AA, Chilukuri S, Shukr N, Fazli Y, Ong N, Afifi ER, Osorio N, Geertsema R, Nesburn AB, Wechsler SL, BenMohamed L. 2015. The herpes simplex virus LAT gene is associated with a broader repertoire of virus-specific exhausted CD8+ T cells retained within the trigeminal ganglia of latently infected HLA transgenic rabbits. J Virol 90:3913–3928. https://doi.org/10.1128/JVI.02450-15.
44. Srivastava R, Khan AA, Huang J, Nesburn AB, Wechsler SL, BenMohamed L. 2015. Herpes simplex virus type 1 human asymptomatic CD8 T cell epitopes protect against ocular herpes in "humanized" HLA transgenic rabbit model. Invest Ophthalmol Vis Sci 56:4013–4028. https://doi.org/10.1167/iovs.15-17074.
45. Srivastava R, Khan AA, Garg S, Syed SA, Furness JN, Vahed H, Pham T, Yu HT, Nesburn AB, BenMohamed L. 2017. Human asymptomatic epitopes identified from the herpes simplex virus tegument protein VP13/14 (UL47) preferentially recall polyfunctional effector memory CD44high CD62Llow CD8+ TEM cells and protect "humanized" HLA-A*02:01 transgenic mice against ocular herpesvirus infection. J Virol 91:e01793-16. https://doi.org/10.1128/JVI.01793-16.
46. BenMohamed L, Osorio N, Khan AA, Srivastava R, Huang L, Krochma JJ, Garcia LM, Simpson JL, Wechsler SL. 2015. Prior corneal scarification and injection of immune serum are not required before ocular HSV-1 infection for UV-B induced virus reactivation and recurrent herpetic corneal disease in latently infected mice. Curr Eye Res 41:747–756. https://doi.org/10.1007/s13365-015-0348-9.
47. BenMohamed L, Osorio N, Srivastava R, Khan AA, Simpson JL, Wechsler SL. 2015. Decreased reactivation of a herpes simplex virus type 1 (HSV-1) latency-associated transcript (LAT) mutant using the in vivo mouse UV-B model of induced reactivation. J Neurovirol 21:508–517. https://doi.org/10.1007/s13365-015-0348-9.
48. Khan AA, Srivastava R, Chentoufi AA, Geertsema R, Thai NT, Dasgupta G, Osorio N, Kalantari M, Nesburn AB, Wechsler SL, BenMohamed L. 2015. Therapeutic immunization with a mixture of herpes simplex virus 1 glycoprotein D-derived "asymptomatic" human CD8+ T-cell epitopes decreases spontaneous ocular shedding in latently infected HLA transgenic rabbits: association with low frequency of local PD-1+ TIM-3+ CD8+ exhausted T cells. J Virol 89:6619–6632. https://doi.org/10.1128/JVI.00788-15.
49. Khan AA, Srivastava R, Chentoufi AA, Kritzer E, Chilukuri S, Garg S, Yu DC, Vahed H, Huang L, Syed SA, Furness JN, Tran TT, Anthony NB, McLaren CE, Sidney J, Sette A, Noelle RJ, BenMohamed L. 2017. Bolstering the number and function of HSV-1-specific CD8+ effector memory T cells and tissue-resident memory T cells in latently infected trigeminal ganglia reduces recurrent ocular herpes infection and disease. J Immunol 199:186–203. https://doi.org/10.4049/jimmunol.1700145.
50. Eckels DD, Gorski J, Rothbard J, Lamb JR. 1988. Peptide-mediated modulation of T-cell allorecognition. Proc Natl Acad Sci U S A 85:8191–8195. https://doi.org/10.1073/pnas.85.21.8191.
51. Kim M, Taylor J, Sidney J, Mikloska Z, Bodsworth N, Lagios K, Dunckley H, Byth-Wilson K, Denis M, Finlayson R, Khanna R, Sette A, Cunningham AL. 2008. Immunodominant epitopes in herpes simplex virus type 2

glycoprotein D are recognized by CD4 lymphocytes from both HSV-1 and HSV-2 seropositive subjects. J Immunol 181:6604–6615. https://doi.org/10.4049/jimmunol.181.9.6604.
52. Hertz T, Yanover C. 2007. Identifying HLA supertypes by learning distance functions. Bioinformatics 23:e148–e155. https://doi.org/10.1093/Bioinformatics/btl324.
53. Botten J, Alexander J, Pasquetto V, Sidney J, Barrowman P, Ting J, Peters B, Southwood S, Stewart B, Rodriguez-Carreno MP, Mothe B, Whitton JL, Sette A, Buchmeier MJ. 2006. Identification of protective Lassa virus epitopes that are restricted by HLA-A2. J Virol 80:8351–8361. https://doi.org/10.1128/JVI.00896-06.
54. Sidney J, Southwood S, Moore C, Oseroff C, Pinilla C, Grey HM, Sette A. 2013. Measurement of MHC/peptide interactions by gel filtration or monoclonal antibody capture. Curr Protoc Immunol Chapter 18:Unit 18.3. https://doi.org/10.1002/0471142735.im1803s100.
55. Vincent A, Willcox N. 1994. Characterization of specific T cells in myasthenia gravis. Immunol Today 15:41–42. https://doi.org/10.1016/0167-5699(94)90027-2.
56. Nagvekar N, Corlett L, Jacobson LW, Matsuo H, Chalkley R, Driscoll PC, Deshpande S, Spack EG, Willcox N. 1999. Scanning a DRB3*0101 (DR52a)-restricted epitope cross-presented by DR3: overlapping natural and artificial determinants in the human acetylcholine receptor. J Immunol 162:4079–4087.
57. Welsh RM, Che JW, Brehm MA, Selin LK. 2010. Heterologous immunity between viruses. Immunol Rev 235:244–266. https://doi.org/10.1111/j.0105-2896.2010.00897.x.
58. Collins N, Jiang X, Zaid A, Macleod BL, Li J, Park CO, Haque A, Bedoui S, Heath WR, Mueller SN, Kupper TS, Gebhardt T, Carbone FR. 2016. Skin CD4$^+$ memory T cells exhibit combined cluster-mediated retention and equilibration with the circulation. Nat Commun 7:11514. https://doi.org/10.1038/ncomms11514.
59. Mackay LK, Rahimpour A, Ma JZ, Collins N, Stock AT, Hafon ML, Vega-Ramos J, Lauzurica P, Mueller SN, Stefanovic T, Tscharke DC, Heath WR, Inouye M, Carbone FR, Gebhardt T. 2013. The developmental pathway for CD103$^+$ CD8$^+$ tissue-resident memory T cells of skin. Nat Immunol 14:1294–1301. https://doi.org/10.1038/ni.2744.
60. Gebhardt T, Wakim LM, Eidsmo L, Reading PC, Heath WR, Carbone FR. 2009. Memory T cells in nonlymphoid tissue that provide enhanced local immunity during infection with herpes simplex virus. Nat Immunol 10:524–530. https://doi.org/10.1038/ni.1718.
61. Reul J, Frisch J, Engeland CE, Thalheimer FB, Hartmann J, Ungerechts G, Buchholz CJ. 2019. Tumor-specific delivery of immune checkpoint inhibitors by engineered AAV vectors. Front Oncol 9:52. https://doi.org/10.3389/fonc.2019.00052.
62. Zens K, Munz C. 2019. Tissue resident T cell memory or how the magnificent seven are chilling in the bone. Eur J Immunol 49:849–852. https://doi.org/10.1002/eji.201948208.
63. Chihara N, Madi A, Kondo T, Zhang H, Acharya N, Singer M, Nyman J, Marjanovic ND, Kowalczyk MS, Wang C, Kurtulus S, Law T, Etminan Y, Nevin J, Buckley CD, Burkett PR, Buenrostro JD, Rozenblatt-Rosen O, Anderson AC, Regev A, Kuchroo VK. 2018. Induction and transcriptional regulation of the co-inhibitory gene module in T cells. Nature 558:454–459. https://doi.org/10.1038/s41586-018-0206-z.
64. Lee H, Heo L, Lee MS, Seok C. 2015. GalaxyPepDock: a protein-peptide docking tool based on interaction similarity and energy optimization. Nucleic Acids Res 43:W431–W435. https://doi.org/10.1093/nar/gkv495.
65. Pos W, Sethi DK, Call MJ, Schulze MS, Anders AK, Pyrdol J, Wucherpfennig KW. 2012. Crystal structure of the HLA-DM-HLA-DR1 complex defines mechanisms for rapid peptide selection. Cell 151:1557–1568. https://doi.org/10.1016/j.cell.2012.11.025.
66. Probst A, Besse A, Favry E, Imbert G, Tanchou V, Castelli FA, Maillere B. 2013. Human CD4 T cell epitopes selective for vaccinia versus variola virus. Mol Immunol 53:453–459. https://doi.org/10.1016/j.molimm.2012.10.011.
67. Castelli FA, Szely N, Olivain A, Casartelli N, Grygar C, Schneider A, Besse A, Levy Y, Schwartz O, Maillere B. 2013. Hierarchy of CD4 T cell epitopes of the ANRS Lipo5 synthetic vaccine relies on the frequencies of pre-existing peptide-specific T cells in healthy donors. J Immunol 190:5757–5763. https://doi.org/10.4049/jimmunol.1300145.
68. Musson JA, Ingram R, Durand G, Ascough S, Waters EL, Hartley MG, Robson T, Maillere B, Williamson ED, Sriskandan S, Altmann D, Robinson JH. 2010. Repertoire of HLA-DR1-restricted CD4 T-cell responses to capsular Caf1 antigen of Yersinia pestis in human leukocyte antigen transgenic mice. Infect Immun 78:4356–4362. https://doi.org/10.1128/IAI.00195-10.
69. Wang XF, Kerzerho J, Adotevi O, Nuyttens H, Badoual C, Munier G, Oudard S, Tu S, Tartour E, Maillere B. 2008. Comprehensive analysis of HLA-DR- and HLA-DP4-restricted CD4$^+$ T cell response specific for the tumor-shared antigen survivin in healthy donors and cancer patients. J Immunol 181:431–439. https://doi.org/10.4049/jimmunol.181.1.431.
70. Texier C, Pouvelle S, Busson M, Herve M, Charron D, Menez A, Maillere B. 2000. HLA-DR restricted peptide candidates for bee venom immunotherapy. J Immunol 164:3177–3184. https://doi.org/10.4049/jimmunol.164.6.3177.
71. Samandary S, Kridane-Miledi H, Sandoval JS, Choudhury Z, Langa-Vives F, Spencer D, Chentoufi AA, Lemonnier FA, BenMohamed L. 2014. Associations of HLA-A, HLA-B and HLA-C alleles frequency with prevalence of herpes simplex virus infections and diseases across global populations: implication for the development of an universal CD8$^+$ T-cell epitope-based vaccine. Hum Immunol 75:715–729. https://doi.org/10.1016/j.humimm.2014.04.016.
72. Zhang X, Dervillez X, Chentoufi AA, Badakhshan T, Bettahi I, Benmohamed L. 2012. Targeting the genital tract mucosa with a lipopeptide/recombinant adenovirus prime/boost vaccine induces potent and long-lasting CD8$^+$ T cell immunity against herpes: importance of MyD88. J Immunol 189:4496–4509. https://doi.org/10.4049/jimmunol.1201121.